Landau theory of the nematic–smectic-A phase transition under shear flow

R. F. Bruinsma
Department of Physics, University of California, Los Angeles, Los Angeles, California 90024
and Institute for Theoretical Physics, University of California, Santa Barbara, Santa Barbara, California 93106

C. R. Safinya
Corporate Research Science Laboratories, Exxon Research and Engineering Company, Annandale, New Jersey 08801
and Institute for Theoretical Physics, University of California, Santa Barbara, Santa Barbara, California 93106
(Received 26 September 1990)

Shear flow distorts the microstructure of fluids if the Deborah number $\mathcal{D}$ becomes comparable to 1. In complex fluids, exotic hydrodynamics effects are often seen in this regime. We compute within Landau theory the structure factor $S(\mathbf{q})$ of a sheared nematic liquid crystal close to the nematic to smectic-A (N–Sm-A) phase transition. As a function of increasing Deborah number, the pretransitional smectic-A fluctuation clusters become increasingly geometrically restricted, evolving from their usual three-dimensional ellipsoidal shape for $\mathcal{D} \ll 1$ to an extremely anisotropic *one-dimensional shape* for $\mathcal{D} \gg 1$. We discuss the predictions of Landau theory for x-ray diffraction experiments for various orientations of the nematic director. The suppression of pretransitional critical fluctuations by shear flow is found to raise the transition temperature $T_{N\text{–Sm-}A}$, and peculiarly, $T_{N\text{–Sm-}A}$ is found to depend on the orientation of the director. The presence of the microscopic fluctuation clusters under the shear flow is also reflected on the macroscopic level. The classical theory of the hydrodynamics of nematic liquid crystals, due to Ericksen, Leslie, and Parodi (ELP), is found to be incomplete. We compute the new fluctuation-induced forces that must be added to ELP nematic hydrodynamics and we discuss their consequence, in particular for large $\mathcal{D}$, the analog of shear-thinning for liquid crystals.

I. INTRODUCTION

The intellectual fascination of scientists with the macroscopic flow behavior of fluids and its relation to the underlying nonequilibrium microscopic structure goes back a century to Reynolds.[1] In principle, the microscopic density-density correlation function $g(r)$ describing the structure of a fluid should experience significant distortions if the Deborah number $\mathcal{D}=\dot{\gamma}\tau$ becomes comparable to one.[2] Here, $\dot{\gamma}$ is the shear rate and τ the longest characteristic structural relaxation time. However, simple fluids (such as water) consist of small molecules with exceedingly fast relaxation times, related to translational and rotational diffusion. The required shear rate would be of order 10^{10}–10^{14} $\sec^{-1}$ which is experimentally not feasible.[3]

High Deborah numbers can be readily achieved in macromolecular liquids (complex fluids) which are liquids with characteristic length scales larger than about 50 Å.[4] This was first demonstrated by Reynolds himself in his studies of the effect of shear flow on a fluid filled with (macroscopic) spheres. Under shear flow the spheres repel each other and order in layers. More recently, Clark and Ackerson[5] have demonstrated the distortions of $g(r)$ in more controlled experiments consisting of charged colloidal suspensions under shear flow where large Deborah numbers can also be reached. Perhaps the best-known case where large Deborah numbers can be realized is that of the flow of polymer fluids.[6] When a rotating rod is inserted in an open beaker containing a concentrated polymeric fluid, the highly "non-Newtonian" fluid is observed to more inwards and to actually climb the rod. This is in contrast with the behavior found for a simple Newtonian fluid, even one which is very viscous such as glycerol, where the fluid surface is depressed near the rod due to centrifugal forces. Polymeric fluids are called non-Newtonian because their shear viscosity is a function of the shear rate; that is, they exhibit either shear thinning or shear thickening. Hydrodynamic descriptions of polymeric fluids exhibiting non-Newtonian behavior must include new terms, the "normal stresses," to account for their rather bizarre macroscopic flow behavior. The microscopic physics of polymer fluids under large Deborah numbers is rather complex, but these non-Newtonian effects are undoubtedly a consequence of complicated structural deformations of the polymer network by the shear flow.

The basic feature of polymeric fluids under shear flow which produces large Deborah numbers and non-Newtonian behavior at low shear rates is the large characteristic length scale for the underlying microscopic structure. For example, the radius of gyration R_G of a polymer is typically of order 100–500 Å. The associated relaxation times τ range between 10^{-5} and 10^{-2} sec for dilute solutions, while they are even larger for concentrated entangled polymeric fluids in the semidilute regime.[7] For a single polymer the characteristic relaxation time τ for chain deformation is of order $\eta R_G^3/k_B T$ (with

 ©1991 The American Physical Society

η the solvent viscosity), so large R_G implies large τ. For the same reason, non-Newtonian effects at experimentally accessible shear rates are also expected for microemulsion spheres and flexible tubes, biological vesicle membranes or tubules, or any complex fluid system with large length and time scales.[4]

An alternative way in which large characteristic length scales can be achieved in fluids occurs spontaneously upon approaching a continuous phase transition where large spatial correlations are built up as a consequence of pretransitional fluctuations. Near the transition, the order-parameter correlation length ξ diverges as $(T-T_c)^{-\nu}$, with T_c the critical temperature. The order-parameter relaxation time τ diverges as ξ^z (critical slowing down).[8] The exponents ν and z depend on the nature of the transition. We thus expect non-Newtonian flow behavior for, say, a binary fluid near its consolute point because of the divergence of τ. Conversely, shear flow should be expected to affect the microscopic structure of a fluid close to its critical point. Because our understanding of physical systems near critical points is often quite complete, we may think of fluids close to their critical point as simple model systems for the investigation of non-Newtonian behavior in complex fluids. The effect of shear flow on critical behavior has been thoroughly explored by Onuki and Kawasaki[9] for binary fluids and among their conclusions were that (i) shear flow suppresses fluctuations, which leads to mean-field critical behavior, and (ii) the spatial correlation function is extremely anisotropic and is quasi-long-ranged along the flow direction. Experimentally,[10] while the mean-field character of the transition has been verified in binary fluids, the quantitative features of $S(\mathbf{q})$ and its evolution with $\dot{\gamma}\tau$ remain unexplored.

We will discuss in this paper the effect of shear flow on the phase transition between the nematic (N) and the smectic-A (Sm-A) phases of liquid crystals.

Liquid crystals can condense in many phases with various degrees of orientational and spatial order of the rod-like organic molecules[11] (see Fig. 1). In the nematic phase the molecules exhibit long-range uniaxial orientational order and short-range positional order. The nematic director $\hat{\mathbf{n}}$, shown schematically in Fig. 1(b), is a unit vector describing the average direction along which the molecules point. By reducing the temperature a transition takes place at $T_{N-\text{Sm-}A}$, into the Sm-A phase. This transition corresponds to the onset of a one-dimensional mass density wave along the director. The Sm-A phase can be thought of as stacks of layers where the molecules are free to diffuse within each two-dimensional sheet [Fig. 1(c)].

Deborah numbers of order 1 have recently been shown to be experimentally accessible,[12] close to the nematic to smectic-A phase transition where we have a detailed understanding of the nature of the pretransitional fluctuations.[13,14] In addition, even away from the critical point the microscopic length scale which is the molecular length is large (of order 30 Å). Thus liquid crystals are suitable systems for investigating the distortions of $g(r)$ by shear flow and the relation with non-Newtonian flow behavior. In particular, liquid crystals could serve as a "laboratory" for developing a microscopic understanding of shear thinning and normal forces.

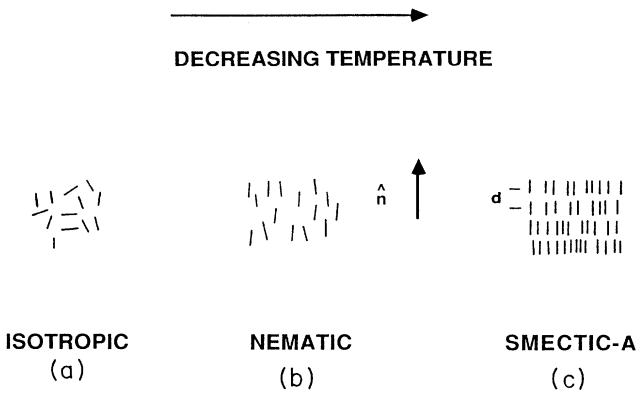

FIG. 1. Schematic representation of three liquid crystalline phases. (a) The isotropic phase of the rod-shaped molecules. (b) The nematic phase exhibits long-range orientational order with the molecules pointing on average along the nematic director $\mathbf{n}$. (c) In the smectic-A phase the molecules segregate into (liquid) layers which are stacked with mean spacing d.

Several authors[15] have theoretically discussed the effect of shear flow on various liquid crystalline phases and phase transitions. de Gennes studied the smectic-A to smectic-C phase transition and found that flow resulted in an interesting anisotropic reduction of the order-parameter fluctuations. Ramaswamy considered the effects of shear flow on the smectic-A phase and found that flow suppresses the order-parameter phase fluctuations and stabilizes the smectic-A phase. In another liquid crystalline system of block copolymers, Fredrickson considered the effects of flow on $S(\mathbf{q})$ in the isotropic phase close to the ordered layered phase which has the same symmetry as the smectic-A phase. He found that for large Deborah numbers, $S(\mathbf{q})$ is highly anisotropic and suppressed. The theory gives an expression for $S(\mathbf{q})$, which when compared to experiments should provide a direct measurement of relaxation times for diblock melts. In a separate study of the isotropic to the lamellar (smectic-A-type) transition in a binary surfactant system, Cates and Milner found that the suppression of fluctuations raises the transition temperature and makes the transition less weakly first order. Olmsted and Goldbart studied the isotropic to nematic transition and discovered remarkably that under flow the transition becomes second order. Larson has considered the steady-state behavior of the nematic director in the nematic phase of flowing liquid-crystal polymers. He finds that in addition to tumbling and steady regimes of the director orientation, a wagging regime may also exist.

The microstructure of liquid crystals can best be probed by x-ray diffraction because x rays couple to density fluctuations. In particular, just above the N–Sm-A transition there are pretransitional Sm-A fluctuations in the nematic phase in the form of correlated clusters with

anisotropic correlation lengths $\xi_{\parallel}$ (along the director) and $\xi_{\perp}$ (perpendicular to the director) [Fig. 2(a)]. The reciprocal space scattering spectrum due to these fluctuations is shown schematically in Fig. 2(b). The fluctuations appear as diffuse scattering spots centered around the points $\pm\mathbf{q}_0=\pm q_0\hat{\mathbf{n}}$. Here, $2\pi/q_0=d$ is the layer spacing of the smectic layers.

The x-ray-scattering structure factor $S(\mathbf{q})$ is proportional to the Fourier transform of the density-density correlation function $g(\mathbf{r})$. The x-ray structure factor of the N–Sm-A transition has been studied extensively[13,14,16] at equilibrium, and it has been found that $S(\mathbf{q})$ is given by an anisotropic Ornstein-Zernike form:[17]

$$S_0(\mathbf{q})=S(\mathbf{q}_0)/[1+\xi_{\parallel}^2(q_z-q_0)^2+\xi_{\perp}^2(q_x^2+q_y^2)] \quad (1.1)$$

where we assumed $\hat{\mathbf{n}}=\hat{\mathbf{z}}$. If $t=(T-T_{N\text{-Sm-}A})/T_{N\text{-Sm-}A}$ is the reduced temperature, then $\xi_{\parallel}$ and $\xi_{\perp}$ diverge near $t=0$, respectively, as $t^{-\nu_{\parallel}}$ and $t^{-\nu_{\perp}}$ with $\nu_{\parallel}>\nu_{\perp}$. In most systems $\nu_{\parallel}$ takes values close to 0.7 and $\nu_{\parallel}-\nu_{\perp}$ is of order 0.15. The anisotropy in the exponents which was initially observed more than a decade ago[13] appears to persist in most systems studied to date.[14] The actual values of $\nu_{\parallel}$ and $\nu_{\perp}$ are theoretically not entirely understood and for the sake of simplicity this anisotropy will be neglected in the present work.[18]

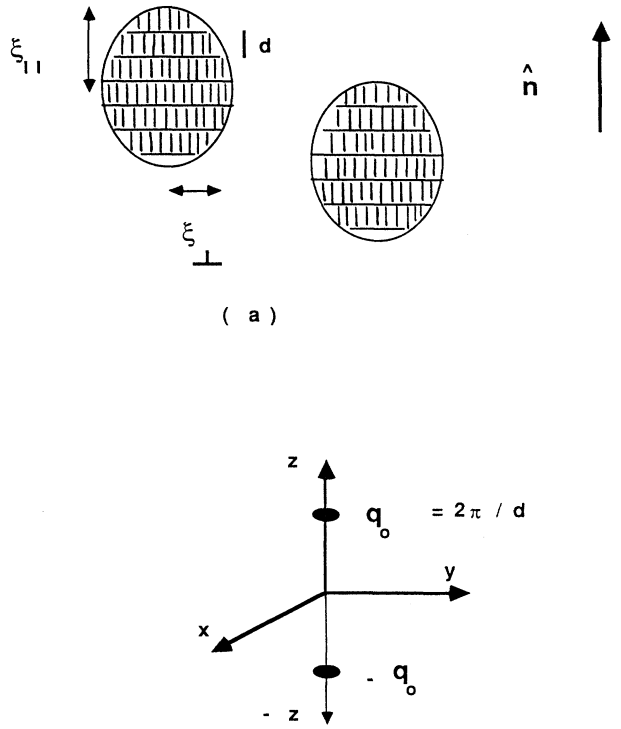

FIG. 2. (a) Real-space schematic of pretransitional smectic-A fluctuation clusters in the nematic phase. Because of the molecular length anisotropy, the domains exhibit anisotropic correlation lengths $\xi_{\parallel}$ (along $\hat{\mathbf{n}}$) and $\xi_{\perp}$ (perpendicular to $\hat{\mathbf{n}}$). (b) The diffuse x-ray scattering in reciprocal space resulting from the fluctuation clusters. The peaks are centers at $\pm 2\pi/d$.

For typical N–Sm-A transitions, the correlation lengths can be quite large, of order 1000 Å at a temperature $t\approx 10^{-4}$ (corresponding to $T-T_{N\text{-Sm-A}}\simeq 30$ mK). The corresponding order-parameter relaxation times are also expected to be greatly increased, and according to ultrasonic absorption and nuclear-magnetic-resonance (NMR) measurements[19] τ should be in the range of 10^{-4} to 10^{-3} sec for $t\approx 10^{-4}$. Therefore, close to the transition, large Deborah numbers could be achieved for shear rates of about 10^4 sec^{-1}, which is indeed accessible in the laboratory.[12] Thus liquid crystals should present suitable systems to study the effect of shear flow on $S(\mathbf{q})$.

There are a number of fundamental differences between the N–Sm-A phase transition and the phase separation transition in binary fluids which require special attention.

(i) The nematic phase is an anisotropic fluid with broken rotational symmetry as characterized by the director $\hat{\mathbf{n}}$. Associated with this broken symmetry are gapless orientational fluctuations[11] ("Goldstone modes") which are responsible for the strong light scattering of nematic liquid crystals.[20]

(ii) The smectic-A phase is at its lower critical dimension in $d=3$; that is, for $d<3$ thermal fluctuations destroy the smectic order.[11,18] Thermal fluctuations in $d=3$ significantly depress the ordering temperature below the mean-field value. This is not the case for binary fluids in $d=3$.

(iii) The smectic-A order parameter does not obey a conservation law. In the binary-fluid case, the order parameter is a conserved quantity.

(iv) In binary fluids $\dot{\gamma}\tau$ is the only control parameter for flow effects to become important. In the N–Sm-A system, because of the large internal length scale d there are *two* relevant parameters whose relative importance depends on the orientation of $\hat{\mathbf{n}}$. When the director points in a plane normal to the flow, $\dot{\gamma}\tau$ is again the only control parameter; whereas when $\hat{\mathbf{n}}$ is along $\mathbf{v}$, $\dot{\gamma}\tau q_0\xi$ becomes the relevant parameter.

Our aim is to understand the N–Sm-A phase transition and how the theory differs from the one described by Kawasaki and Onuki in view of (i)–(iv). We now discuss our results, which can be summarized by first considering the correlation function $S(\mathbf{q})$ and then its effect on the macroscopic response parameters.

We find that for small Deborah numbers ($\dot{\gamma}\tau\ll 1$), the effect of shear flow on the structure factor can be described as a *shear* of the fluctuation clusters. More explicitly if $\mathbf{v}=\dot{\gamma}y\hat{\mathbf{x}}$ is the flow velocity, we find that

$$S(\mathbf{q})\simeq S_0(q_x,q_y+\dot{\gamma}\tau(\mathbf{q})q_x,q_z), \quad \dot{\gamma}\tau(\mathbf{q})\lesssim 1 \quad (1.2)$$

where $\tau(\mathbf{q})=(\gamma_3/k_BT)S_0(\mathbf{q})$ is the $\mathbf{q}$-*dependent* order-parameter relaxation time (γ_3 is a viscosity). Equation (1.2) corresponds to a shear of $S_0(\mathbf{q})$ in the q_x-q_y plane by an amount $\dot{\gamma}\tau(\mathbf{q})$. The effect of larger shear rates on $S(\mathbf{q})$ is best discussed by first recalling the dynamical scaling

argument.[8] This will also highlight the importance of conservation laws mentioned earlier for the response to shear flow of a critical system.

According to dynamical scaling, the wave-vector-dependent order-parameter relaxation rate $\omega(q)$ obeys

$$\omega(q)=q^z\Omega(q\xi) . \tag{1.3}$$

For a nonconserved two-component order parameter,[8] $z=\frac{3}{2}$ and the function $\Omega(x)\sim 1/x^z$ for $x\ll 1$ while $\Omega(x)$ goes to a constant for $x\gg 1$. We expect that when $\omega(q)>\dot\gamma$, the fluctuations will dissipate thermally before the imposed flow field can distort them, while for $\omega(q)<\dot\gamma$ the fluctuations are distorted before they decay. It follows from Eq. (1.3) that $\omega(q)\propto 1/\xi^z$ for $q\xi\ll 1$ while $w(q)\propto q^z$ for $q\xi\gg 1$. Figure 3 is a schematic plot of $\omega(q)$ versus q for a nonconserved order parameter. We see that if $\dot\gamma<\omega(0)$ (dashed line), we are in the small Deborah number regime for *all* q since $\omega(q)>\dot\gamma$. Little effect is expected on $S(\mathbf{q})$ in this regime. On the other hand, if $\dot\gamma>\omega(0)$ then there will be a *range of wave vectors* for which $\dot\gamma>\omega(q)$. Therefore, for $\dot\gamma>\omega(0)$, we can introduce a length scale q_s (see Fig. 3):

$$\omega(q_s)=\dot\gamma \tag{1.4a}$$

or, using the large x behavior of $\Omega(x)$,

$$q_s(\dot\gamma)\propto\dot\gamma^{\,1/z} . \tag{1.4b}$$

The wave vector $\mathbf{q}_s$ defines a sphere in $\mathbf{q}$ space, such that for $|\mathbf{q}|>|q_s(\dot\gamma)|$, $S(\mathbf{q})$ must be undistorted while for $|\mathbf{q}|<|q_s(\dot\gamma)|$, $S(\mathbf{q})$ should be distorted. Thus all order-parameter fluctuations with $\xi>q_s^{-1}$ are expected to be distorted due to shear flow. The condition that $\dot\gamma$ should exceed $\omega(0)$ in order for us to see significant distortions in $S(\mathbf{q})$ is actually just our previous criterion that the Deborah number $\dot\gamma\tau$ must exceed 1. For a conserved order parameter $\omega(q)\to 0$ for $q\to 0$,[8] so that for all small but finite shear rates, there is always a range of wave vectors for which $\dot\gamma>\omega(q)$ and shear has an effect.

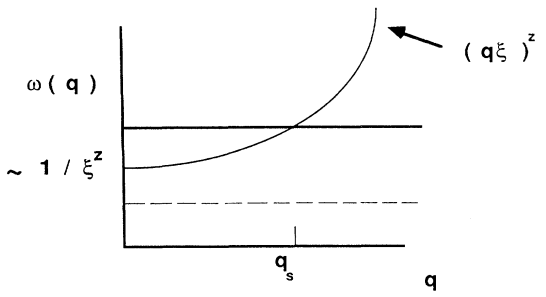

FIG. 3. The order-parameter decay rate $\omega(q)$ vs q for a nonconserved order parameter plotted schematically at a temperature $T>T_{N\text{-Sm-}A}$ so that ξ is finite. If $\dot\gamma<\omega(0)$ (dashed line), then $\dot\gamma<\omega(q)$ for all q and shear will not effect $S(\mathbf{q})$. On the other hand, if $\dot\gamma>\omega(0)$ (bold line) then $\dot\gamma>\omega(q)$ for all $q<q_s(\dot\gamma)$ and are effected by shear. Note that for a conserved order-parameter system (e.g., binary fluid) $\omega(0)=0$ so that for any finite $\dot\gamma$ there is a range of q's that are affected by flow.

While the preceding argument is correct for a nonconserved order parameter with isotropic order-parameter fluctuations, we shall see that for the N–Sm-A transition with anisotropic fluctuations, $\mathbf{q}_s$ will be anisotropic in all three directions. We find that in the distorted regions in $\mathbf{q}$ space, the spatial density-density correlations exhibit quasi-long-range order along the flow direction and are cut off in the plane normal to the flow. That is, the fluctuation clusters which are ellipsoidal at $\dot\gamma=0$ now become elongated and oriented along the flow.

In momentum space, this elongation leads to a *power-law behavior* for $S(\mathbf{q})$ in the distorted region:

$$S(\mathbf{q})\propto 1/(\dot\gamma^{\,2}q_x^2)^{1/3} \quad \text{for} \quad \begin{cases}\dot\gamma\tau\gg 1, & \hat n\perp\mathbf{v}\\ \dot\gamma\tau q_0\xi_\perp\gg 1, & \hat n\parallel\mathbf{v}\end{cases} . \tag{1.5}$$

Equation (1.5) signifies that for extremely large Deborah numbers, the density-density correlations along the flow are qualitatively different than at $\dot\gamma=0$, and exhibit quasi-long-range order. We can now apply Eqs. (1.2) and (1.5) to the fluctuations $\langle|\psi|^2\rangle$ of the smectic-A order parameter in the nematic phase:

$$\langle|\psi|^2\rangle=\int d^3q\, S(\mathbf{q}) . \tag{1.6}$$

For $\dot\gamma\tau\ll 1$, $\langle|\psi|^2\rangle$ is unaffected by shear flow but for $\dot\gamma\tau\gg 1$, $\langle|\psi|^2\rangle$ vanishes as $\dot\gamma^{\,-2/3}$. Because of this suppression of thermal fluctuations, $d=3$ smectic liquid crystals are in fact no longer at their lower critical dimension for $\dot\gamma\neq 0$. As noted, the suppression by shear flow of fluctuations also occurs in binary fluids.

We now turn to the macroscopic physics. A number of macroscopic response parameters can be expressed in terms of $S(\mathbf{q})$ and are thus strongly affected by the suppression of $S(\mathbf{q})$ for $\dot\gamma\tau(\mathbf{q})\gg 1$. Also, as expected from our experience with non-Newtonian fluids, we find surprising dynamical effects.

(I) The classical equations of motion of the nematic director coupled to flow were constructed based on a macroscopic theory of anisotropic fluids by Ericksen,[21] Leslie,[22] and Parodi[23] (ELP). An alternate description, which emphasizes correlation functions, was later developed by Foster *et al.* and by Martin, Parodi, and Pershan.[24] According to ELP nematic hydrodynamics, the director is (nearly) aligned along the flow ($\hat{\mathbf{x}}$) direction when the Leslie viscosity parameter α_3 ($\propto\eta_b$) is negative—which is the case far above $T_{N\text{-Sm-}A}$. (Figure 4 shows the nematic geometry for the three viscosities η_a, η_b, and η_c: η_b is for $\hat{\mathbf{n}}$ parallel to $\mathbf{v}$ and η_a and η_c for $\hat{\mathbf{n}}$ perpendicular to $\mathbf{v}$.[25]) For α_3 positive (which is true closer to $T_{N\text{-Sm-}A}$) $\hat{\mathbf{n}}$ precesses around the $\hat{\mathbf{z}}$ axis [neutral direction, see Fig. 4(a)]. It was demonstrated by McMillan[26] and by Janig and Brochard[27] that in the presence of smectic fluctuations, ELP nematic hydrodynamics retains its validity for low shear rates if we renormalize the viscosity parameter α_3.

We find that *even for reasonably small Deborah numbers* (i.e., $\dot\gamma\tau<1$) *ELP nematic hydrodynamics is incomplete.* The flow distortion of $S(\mathbf{q})$ creates a "normal"

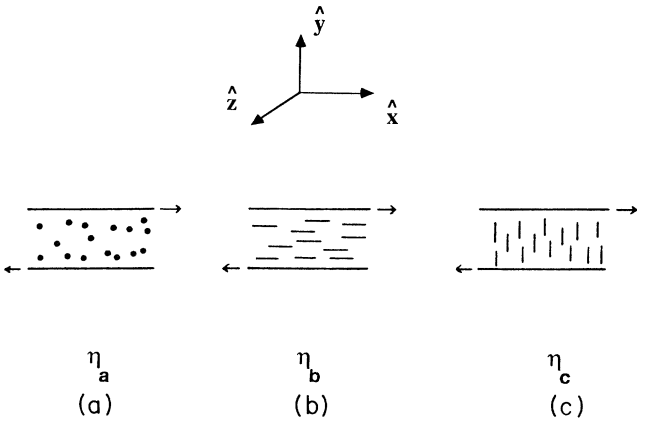

FIG. 4. Three fundamental geometries for the nematic viscosities. (a) η_a is the viscosity with the director perpendicular to the shear flow (x-y) plane. (b) η_b is the viscosity with the director along the velocity ($\hat{\mathbf{x}}$) direction. (c) η_c is the viscosity with the director along the velocity gradient ($\hat{\mathbf{y}}$) direction.

torque $\hat{\mathbf{n}}\times\mathbf{h}$, with $\mathbf{h}\cong-(\gamma_1^R/\tau_N)n_x\hat{\mathbf{x}}$ on the director which cannot be absorbed by a redefinition of the Leslie parameters (γ_1^R is again a viscosity). For small $\dot{\gamma}\tau$,

$$\tau_N^{-1}\cong\frac{1}{96\pi}\frac{(\dot{\gamma}\tau)^2}{\gamma_1^R\xi_\parallel}q_0^2k_BT\ . \tag{1.7}$$

This normal torque is intimately related to the effect of shear flow on the Goldstone modes of the nematic phase. Shear flow destroys the rotational symmetry so the dispersion relation ω_q of the orientational fluctuations acquires a gap. For $\hat{\mathbf{n}}=\hat{\mathbf{z}}$, we find for the mode spectrum

$$\omega^{\pm}(\mathbf{q})=i\left[\frac{Kq^2}{\gamma_1^R}+\frac{1}{2\tau_N}\right]\pm\left[\omega_0^2-\left[\frac{1}{2\tau_N}\right]^2\right]^{1/2}, \tag{1.8}$$

where $\omega_0=(\dot{\gamma}/\gamma_1^R)(-\alpha_2\alpha_3^R)^{1/2}$. The (negative) quantity α_2 is another Leslie parameter and K is a Frank stiffness constant. According to Eq. (1.8), both the real and imaginary parts of the spectrum have a gap for $\dot{\gamma}\neq0$. $\mathrm{Re}\omega(\mathbf{q})\approx\pm\omega_0$ with ω_0 the precession frequency of the director for $\dot{\gamma}\to0$, while $\mathrm{Im}\omega(0)=\frac{1}{2}\tau_N^{-1}$ if the precession is underdamped.

(II) At zero shear rate, the nematic bend and twist elastic constants[20,28,29] K_2 and K_3 as well as the viscosity coefficient[26,27,30,31] η_b diverge near $T_{N\text{-Sm-}A}$ because of the fluctuation renormalization effects.

Because shear flow reduces thermal fluctuations the fluctuation corrections are also eliminated at high shear rates. The suppression of fluctuations is found, however, to be very dependent on the angle between the flow direction (along $\hat{\mathbf{x}}$) and the nematic director. As a consequence, *the response coefficients* η_b, K_2, and K_3 *must depend strongly on* $\hat{\mathbf{n}}$ *in shear flow.* For instance, for the Leslie parameter α_3 (which is proportional to η_b) we find that

$$\alpha_3\simeq\begin{cases}\alpha_3^R(\dot{\gamma}=0), & \dot{\gamma}\tau\ll1,\ \hat{\mathbf{n}}=\hat{\mathbf{z}}\\ \alpha_3, & \dot{\gamma}\tau\gg1,\ \hat{\mathbf{n}}=\hat{\mathbf{z}}\end{cases} \tag{1.9a}$$

and

$$\alpha_3\simeq\begin{cases}\alpha_3^R(\dot{\gamma}=0), & \dot{\gamma}\tau q_0\xi\ll1,\ \hat{\mathbf{n}}=\hat{\mathbf{x}}\\ \alpha_3, & \dot{\gamma}\tau q_0\xi\gg1,\ \hat{\mathbf{n}}=\hat{\mathbf{x}}\ .\end{cases} \tag{1.9b}$$

Here, α_3 is the "bare" value of the Leslie viscosity parameter [$\alpha_3<0$ (Ref. 32)] while $\alpha_3^R(\dot{\gamma}=0)$ is the renormalized value in the absence of shear flow [$\alpha_3^R(\dot{\gamma}=0)>0$ close to $T_{N\text{-Sm-}A}$]. Shear flow reduces the viscosity from $\alpha_3^R(\dot{\gamma}=0)$ to α_3. A similar suppression of the renormalized elastic constants K_2 and K_3 is found. The anisotropy of α_3^R has surprising consequences. According to Eq. (1.9), there is for $q_0\xi\gg1$ (i.e., close to $T_{N\text{-Sm-}A}$) a range of shear rates ($1/q_0\xi\lesssim\dot{\gamma}\tau\lesssim1$) where $\alpha_3^R(\dot{\gamma})$ is positive for $\hat{\mathbf{n}}$ along the $\hat{\mathbf{z}}$ direction but negative for $\hat{\mathbf{n}}=\hat{\mathbf{x}}$. This means that *both* the $\hat{\mathbf{n}}=\hat{\mathbf{x}}$ and $\hat{\mathbf{n}}=\hat{\mathbf{z}}$ orientations are stable in this range. We thus expect that in this range the director texture will contain domains with $\hat{\mathbf{n}}\approx\hat{\mathbf{x}}$ and $\hat{\mathbf{n}}\approx\hat{\mathbf{z}}$ separated by domain walls.

(III) For $\mathbf{v}=\dot{\gamma}y\hat{\mathbf{x}}$, the so-called "first normal-stress coefficient" N_1 is defined as $N_1=(\sigma_{xx}-\sigma_{yy})/\dot{\gamma}^2$, with σ_{ij} the stress tensor. We find that near $T_{N\text{-Sm-}A}$

$$N_1\propto\left[\frac{\tau^2}{\xi_\parallel\xi_\perp}\right]k_BT\ . \tag{1.10}$$

Within mean-field theory, N_1 diverges as $1/(T-T_{N\text{-Sm-}A})^{1/2}$. The appearance of normal stresses is one of the characteristics of non-Newtonian liquids. We saw already from Eq. (1.9) that shear flow leads to shear thinning in the α_3^R viscosity (the other characteristic). We thus conclude that near $T_{N\text{-Sm-}A}$, a nematic liquid crystal may show the flow behavior of a non-Newtonian fluid.

(IV) For low shear rates, shear flow increases the phase-transition temperature $T_{N\text{-Sm-}A}(\dot{\gamma})$. Defining the reduced temperature $t(\dot{\gamma})\equiv[T_{N\text{-Sm-}A}(\dot{\gamma})-T_{N\text{-Sm-}A}(0)]/T_{N\text{-Sm-}A}(0)$, we find

$$t(\dot{\gamma})\propto(\dot{\gamma}\tau)^2/\xi \tag{1.11}$$

for $\hat{\mathbf{n}}=\hat{\mathbf{z}}$. Because of flow-induced mixing, shear flow *reduces* the critical temperature of binary mixtures. Similar to our results, Cates and Milner[15] have found that in lyotropic systems the isotropic-to-lamellar phase-transition temperature increases as well under shear flow.

The plan of our paper is as follows. In Sec. II we derive a number of results from a simple geometrical argument which can predict the qualitative features of the x-ray structure factor for smaller Deborah numbers. In Sec. III we present a time-dependent Landau theory of the N–Sm-A transition under shear flow. The results obtained through the geometrical arguments of Sec. II are derived quantitatively and $S(\mathbf{q})$ is derived for large Deborah numbers. In Sec. IV we consider nematic hydrodynamics in the presence of fluctuations (i.e., critical hydrodynamics) and Sec. V discusses our conclusions.

II. SHEARED FLUCTUATION CLUSTERS

We will discuss separately the three director orientations $\hat{\mathbf{n}}=\hat{\mathbf{z}}$, $\hat{\mathbf{n}}=\hat{\mathbf{y}}$, and $\hat{\mathbf{n}}=\hat{\mathbf{x}}$. First consider a fluctuation cluster with $\hat{\mathbf{n}}=\hat{\mathbf{z}}$, so the director is perpendicular to the x-y shear plane. The flow direction is presumed to be along $\hat{\mathbf{x}}$ and the flow gradient along $\hat{\mathbf{y}}$ [Fig. 4(a)]. For zero shear, a fluctuation domain has a circular cross section in the x-y plane with a radius of order $\xi_\perp$ [Fig. 5(a)]. If we switch on the shear flow then the flow will shear the circle into an ellipse [Fig. 5(b)]. Since the fluctuation domain has only a finite lifetime τ, the domain will be sheared by only a finite amount. If $\dot{\gamma}=\partial v_x/\partial y$ is the shear rate, then over the lifetime τ imposed on the cluster, the relative sliding motion of x-z planes imposed by the flow will result in a shear strain of the cluster of the order of $\epsilon=\dot{\gamma}\tau$ along $\hat{\mathbf{x}}$. Therefore the flow field translates each point (x,y) in the circle to a new point $(x',y')=(x+\epsilon y,y)$. The sheared cross section of the domain will thus be given by

$$\frac{(x-\dot{\gamma}\tau y)^2}{\xi_\perp^2}+\frac{y^2}{\xi_\perp^2}=1 \ . \tag{2.1}$$

This describes an ellipse whose long axis makes an angle

$$\phi=\tfrac{1}{2}\tan^{-1}(2/\dot{\gamma}\tau) \tag{2.2}$$

with the $\hat{\mathbf{x}}$ axis [Fig. 5(b)]. The long and short axes ξ^+ and ξ^- are

$$\frac{\xi^\pm}{\xi_\perp}=\left[\frac{2+(\dot{\gamma}\tau)^2\mp[(\dot{\gamma}\tau)^4+4(\dot{\gamma}\tau)^2]^{1/2}}{2}\right]^{-1/2} . \tag{2.3}$$

A shear flow may be described by a strain-rate tensor which can be decomposed[2] as a pure vorticity $\boldsymbol{\omega}=\frac{1}{2}(\nabla\times\mathbf{v})$ and a symmetric part $A_{ij}=\frac{1}{2}(\partial v_i/\partial x_j+\partial v_j/\partial x_i)$. The only nonzero terms in A_{ij} are $A_{xy}=A_{yx}=\frac{1}{2}\dot{\gamma}$ and this causes an elongation in the x-y plane along an angle of $\pi/4$ with the x axis. At low shear rates the elongation dominates over the rotation so ϕ should be $\pi/4$, while, with increasing $\dot{\gamma}$, ϕ should be reduced due to the vorticity to $\phi=0$. We indeed have from Eq. (2.2) that as $\dot{\gamma}\tau\to 0$, $\phi\to\pi/4$. In the opposite limit ($\dot{\gamma}\to\infty$), $\phi\to 0$ and

$$\xi^+/\xi_\perp\simeq\dot{\gamma}\tau \ , \tag{2.4}$$

$$\xi^-/\xi_\perp\simeq 1/\dot{\gamma}\tau \ . \tag{2.5}$$

We plot, in Fig. 6, the alignment angle ϕ and the correlation lengths as a function of the shear. For large $\dot{\gamma}\tau$, the fluctuation cluster is an extremely elongated ellipse oriented along the $\hat{\mathbf{x}}$ direction, with extended correlation lengths along the flow direction ($\xi^+\gg\xi_\perp$), and suppressed correlations along directions perpendicular to the flow direction ($\xi^-\ll\xi_\perp$) as expressed by Eqs. (2.4) and (2.5). This enhancement of correlations along the flow direction is an analog of the shear ordering discovered by Reynolds.[1]

We should point out two basic assumptions that went into this argument. We assumed (i) that the relaxation time τ was a constant independent of the amount of shear distortion, and (ii) that the flow field is always that of simple shear undistorted by the fluctuation clusters. The limiting angle ϕ for large $\dot{\gamma}\tau$ is only zero if τ is indeed independent of $\dot{\gamma}$. We expect that actually τ will decrease substantially for large $\dot{\gamma}\tau$, since the diffusion of molecules out of the cluster into the nematic background would be facilitated by elongation. It is also important to realize that fluctuation clusters in a nematic matrix are not to be considered as drops with a finite surface tension. In that case, the elongated cluster would break up into smaller clusters due to the surface tension. The fluctuation cluster is a region where one has locally increased smecticlike correlations; the cluster has no sharp boundaries.

We now turn to x-ray diffusion. For $\dot{\gamma}=0$ and $\hat{\mathbf{n}}=\hat{\mathbf{z}}$, there are two diffuse scattering maxima at $\pm q_0\hat{\mathbf{z}}$ [Fig. 2(b)]. However, because the clusters are anisotropic with $\xi_\parallel>\xi_\perp$, the structure factor $\mathbf{S}(q)$ (which is proportional to

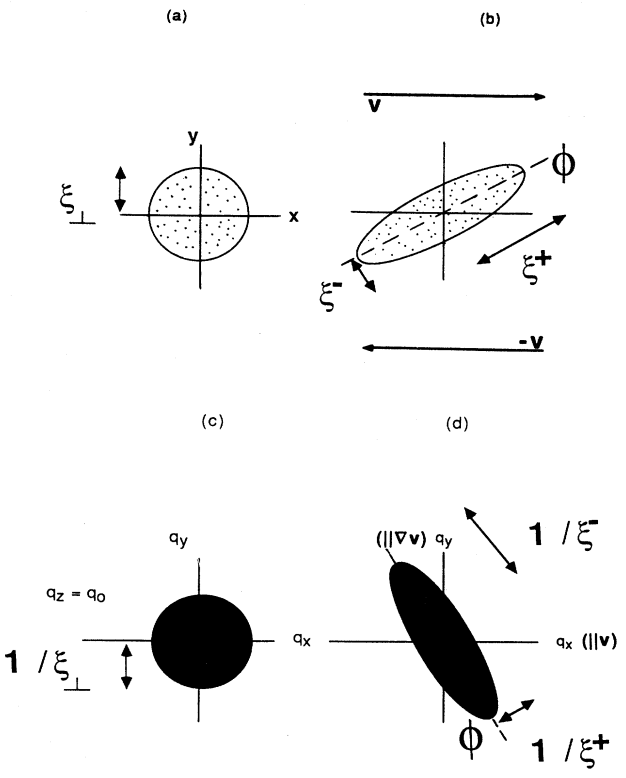

FIG. 5. (a) Isotropic cross section of a fluctuation cluster in the x-y plane with the director along $\hat{\mathbf{z}}$ under static conditions with $\dot{\gamma}=0$. (b) The same cluster under simple shear flow ($\mathbf{v}=\dot{\gamma}y\hat{\mathbf{x}}$, $\dot{\gamma}$ is the shear rate) with the Deborah number $\mathcal{D}(=\dot{\gamma}\tau)>1$. The flow field shears the cluster resulting in an elongated elliptical cluster with long and short axes ξ^+ and ξ^- and orientation angle ϕ as discussed in the text. (c) and (d) Schematics of the x-ray diffuse scattering in reciprocal space resulting from the cluster at rest (c) and the cluster under shear flow (d). The effective sizes of the x-ray-scattering regions in reciprocal space are the inverse of the sizes in real space.

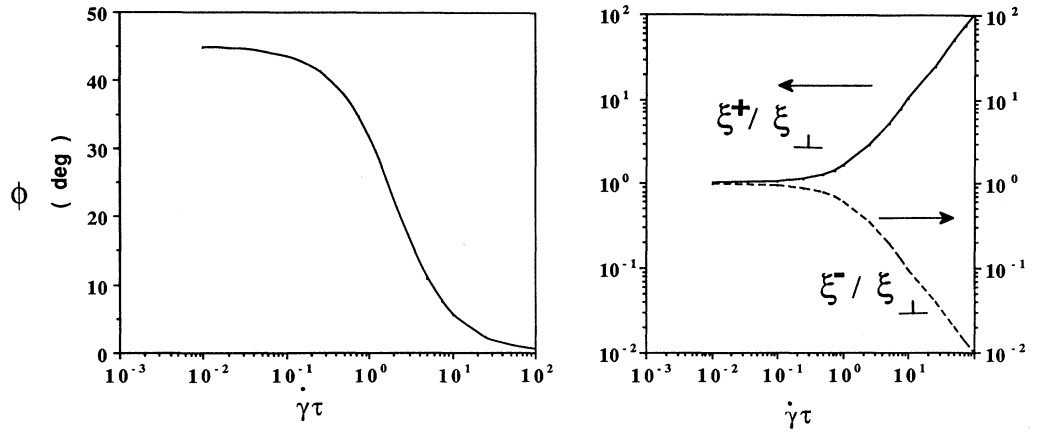

FIG. 6. The alignment angle ϕ and the correlation lengths ξ^+ and ξ^- of the cluster [Figs. 5(a) and 5(b)] as a function of the Deborah number $\mathcal{D}$. The regime of interest corresponds to $\mathcal{D}>1$ which describes the evolution of the cluster from an isotropic shape towards a highly distorted elongated ellipse aligned along the flow direction.

the Fourier transform of the density-density correlation function) is also anisotropic and given by Eq. (1.1) [see Fig. 2(b)]. The $S(\mathbf{q})$=const contour is an ellipsoid in reciprocal space centered about $\pm q_0\hat{\mathbf{z}}$. The short axis is of order $\xi_\parallel^{-1}$ while the two long axes are of order $\xi_\perp^{-1}$. The size of the scattering ellipsoid in $\mathbf{q}$ space is roughly the inverse of the size of the cluster in real space and the $\mathbf{q}$-space ellipsoid is rotated over $\pi/2$ about the $\hat{\mathbf{z}}$ axis as compared to the real-space cluster. For $\dot\gamma\neq 0$ the cluster has an elliptical cross section in the x-y plane, as discussed previously, with dimensions ξ^+ and ξ^- and orientation ϕ [Fig. 5(b)]. Therefore we expect that the $S(\mathbf{q})$=const contour lines define an ellipse in $\mathbf{q}$ space with long axis $(\xi^-)^{-1}$ and short axis $(\xi^+)^{-1}$ oriented at an angle $\phi+\pi/2$ with the flow ($\hat{\mathbf{x}}$) direction. Alternatively, since the sheared fluctuation cluster in real space [Fig. 5(b)] is created by shearing by an amount $\dot\gamma\tau$ along $\hat{\mathbf{x}}$ we expect that in momentum space we should find $S(\mathbf{q})$ by a shear of $-\dot\gamma\tau$ along the q_y direction. (This is because the shear operator $y\partial/\partial x$ in real space acts as $-q_x\partial/\partial q_y$ in momentum space.) The result of such a shear in momentum space is shown in Fig. 5(d). The argument thus predicts that

$$S(\mathbf{q})_{\dot\gamma\neq 0}\simeq S_{\dot\gamma=0}(q_x,q_y+\dot\gamma\tau q_x,q_z)\ , \tag{2.6}$$

which indeed describes an ellipse in $\mathbf{q}$ space rotated by $\pi/2$ compared with the ellipse in real space. The importance of Eq. (2.6) lies in the fact that it would provide us with a very direct way of measuring the Deborah number by x-ray diffraction. At present, we do not have a very reliable way of measuring the Deborah number. In the following section we will show that Eq. (2.6) should indeed be valid at small Deborah numbers when τ is replaced by $\tau(\mathbf{q})$.

Next, we take $\hat{\mathbf{n}}$ along the $\hat{\mathbf{y}}$ axis as in Fig. 7(a). A fluctuation cluster, sheared along $\hat{\mathbf{x}}$ by $\dot\gamma\tau$, can then be defined by

$$\left[\frac{x-\dot\gamma\tau y}{\xi_\perp}\right]^2+\left[\frac{y}{\xi_\parallel}\right]^2=1 \tag{2.7}$$

as shown in Fig. 7(b). The axes of the ellipse are

$$\xi^\pm=\left[\frac{\frac{1}{\xi_\parallel^2}+\frac{1}{\xi_\perp^2}+\left[\frac{\dot\gamma\tau}{\xi_\perp}\right]^2\mp\left[\left[\frac{\dot\gamma\tau}{\xi_\perp}\right]^4+2\left[\frac{\dot\gamma\tau}{\xi_\perp}\right]^2\left[\frac{1}{\xi_\parallel^2}+\frac{1}{\xi_\perp^2}\right]+\left[\frac{1}{\xi_\parallel^2}-\frac{1}{\xi_\perp^2}\right]^2\right]^{1/2}}{2}\right]^{-1/2}\ . \tag{2.8}$$

In reciprocal space, Eq. (2.7) defines an ellipse centered at $q_0\hat{\mathbf{y}}$, elongated (roughly) along the q_y direction. The correlation lengths ξ^+ and ξ^- in the limit $\dot\gamma\tau\to\infty$ are, from Eq. (2.8), as before

$$\xi^+/\xi_\parallel\simeq\dot\gamma\tau\ , \tag{2.9a}$$

$$\xi^-/\xi_\perp\simeq 1/\dot\gamma\tau\ , \tag{2.9b}$$

while $\phi\to 0$ as $\dot\gamma\tau\to\infty$.

In the limit of small shears we find

$$\xi^+\to\xi_\parallel\left[1+\frac{\xi_\parallel^2}{2(\xi_\parallel^2-\xi_\perp^2)}(\dot\gamma\tau)^2\right]\ , \tag{2.10a}$$

$$\xi^-\to\xi_\perp\left[1-\frac{\xi_\parallel^2}{2(\xi_\parallel^2-\xi_\perp^2)}(\dot\gamma\tau)^2\right]\ , \tag{2.10b}$$

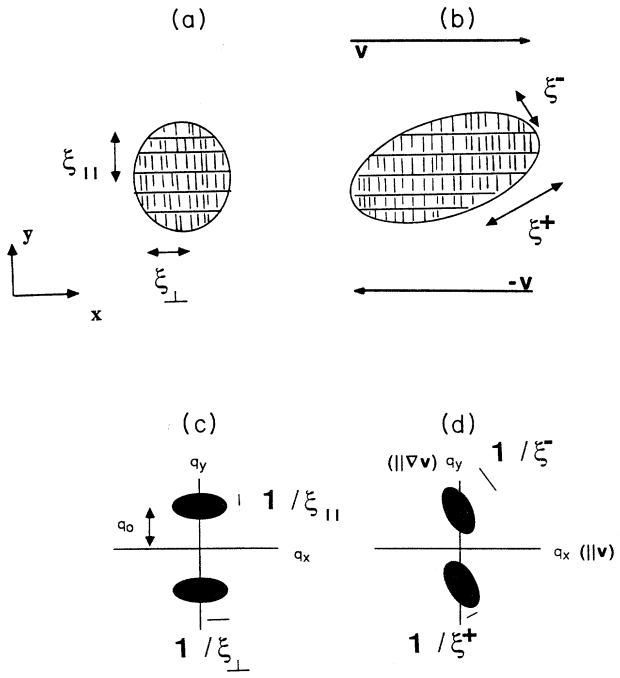

FIG. 7. (a) and (b) Schematic of an anisotropic cluster with the nematic director $\hat{\mathbf{n}}$ along $\hat{\mathbf{y}}$, at rest (a), and under shear flow with $\mathcal{D}>1$ (b). (c) and (d) Schematic of the diffuse scattering in reciprocal space arising from the anisotropic cluster at rest (a), and under shear flow (b).

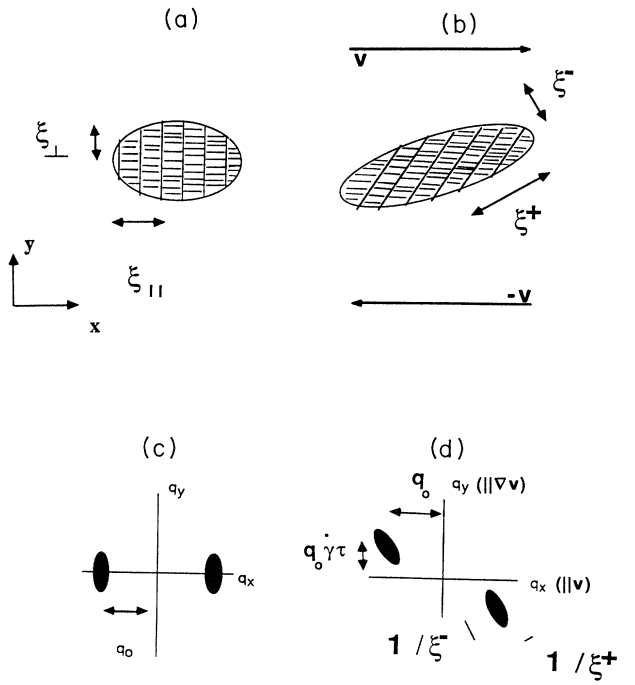

FIG. 8. (a) and (b) Schematic of an anisotropic cluster with the nematic director along $\hat{\mathbf{x}}$ (the flow direction) at rest (a), and under shear flow with $\mathcal{D}>1$ (b). For this orientation of the director the smectic layers are tilted which results in a decrease of the mean interlayer spacing. (c) and (d) Schematic of the diffuse scattering in reciprocal space arising from the anisotropic cluster at rest (a), and under shear flow (b). The tilting of the layers in real space shifts the peaks from their equilibrium positions along the x axis at $\pm q_0\hat{\mathbf{x}}$, to off-axis peaks running off to $\pm\infty$ as $\mathcal{D}$ tends to ∞.

while $\phi\rightarrow\pi/2$. (In the limit that $\xi_{\parallel}=\xi_\perp$ for small shears, $\xi^{\pm}\rightarrow\xi_\perp[1\pm(\dot{\gamma}\tau)/2]$.)

Finally, consider a fluctuation cluster with $\hat{\mathbf{n}}=\hat{\mathbf{x}}$, aligned along the flow direction as in Fig. 8(a). This configuration has very interesting features. For $\dot{\gamma}=0$, the smectic layers of course are parallel to the y-z plane and spaced by $2\pi/q_0$ [Fig. 8(a)], but after shearing the cluster [Fig. 8(b)], the layers are rotated over an angle

$$\theta=\arctan(\dot{\gamma}\tau)\ . \tag{2.11}$$

The long and short axes are found from Eq. (2.8) by exchanging $\xi_{\parallel}$ and $\xi_\perp$. With $\hat{\mathbf{n}}$ fixed along $\hat{\mathbf{x}}$, this rotation means that the layer spacing is reduced to $(2\pi/q_0)\cos\theta$. The shear flow has severely distorted the internal structure of the fluctuation cluster. Obviously, this configuration will be energetically more costly than the two previous configurations. We thus expect that the director will feel a torque trying to twist it out of this configuration. We will discuss this torque in detail in Sec. IV. The shape of the fluctuation cluster under flow in the x-y plane is again an ellipse [Fig. 8(b)],

$$\frac{(x-\dot{\gamma}\tau y)^2}{\xi_{\parallel}^2}+\left[\frac{y}{\xi_\perp}\right]^2=1\ . \tag{2.12}$$

We now turn to the diffraction spots. For $\dot{\gamma}=0$, the scattering maxima are at $\pm q_0\hat{\mathbf{x}}$ [Fig. 8(c)]. Under shear flow, the tilt of layers means that the peaks move off the q_x axis and acquire a q_y component with $q_y=-q_0\dot{\gamma}\tau$. Consequently, the new peak positions $\mathbf{q}^*$ will be [Fig. 8(d)]

$$\mathbf{q}^*=\pm q_0(1,-\dot{\gamma}\tau,0)\ . \tag{2.13}$$

Since under shear flow these pretransitional fluctuations are energetically costly, we expect that the diffraction intensity will be very weak in this configuration.

In summary, the orientation with the nematic director $\mathbf{n}$ along the flow direction should lead to diffraction intensities which are very different from those where $\mathbf{n}$ is perpendicular to $\mathbf{v}$. With $\mathbf{n}$ parallel to $\mathbf{v}$, the smectic fluctuations are strongly suppressed, and the scattering maximum is greatly displaced. With $\mathbf{n}$ perpendicular to $\mathbf{v}$, the scattering maximum should not be much affected by shear flow, while $S(\mathbf{q})$ should acquire a quasi-one-dimensional character for nonzero q_x.

For general orientations of $\hat{\mathbf{n}}$, we would expect that for $\hat{\mathbf{n}}\perp\mathbf{v}$, there is a scattering maximum in $S(\mathbf{q})$ at $q_0\hat{\mathbf{n}}$ in the q_y-q_z plane. Along the q_x direction $S(\mathbf{q})$ is expected to

have quasi-one-dimensional behavior for large $\dot{\gamma}\tau$. If $\hat{\mathbf{n}}$ is not perpendicular to $\mathbf{v}$, then for large $\dot{\gamma}\tau$, the scattering maximum will move to infinity and fluctuations are again suppressed.

III. TIME-DEPENDENT LANDAU THEORY

The Landau theory of the continuous transition between the nematic and smectic-A phases in the absence of shear flow was constructed by de Gennes[28] and McMillan.[29] It predicts a pretransitional increase in certain elastic constants of the nematic phase which indeed has been observed.[20] Similarly, pretransitional fluctuations renormalize the viscosities of the nematic phase.[30,31] This is due to the fact that, as we saw, fluctuation clusters prefer the orientation with $\hat{\mathbf{n}}\perp\mathbf{v}$. The nematic viscosity with $\hat{\mathbf{n}}$ parallel to $\mathbf{v}$ (η_b) indeed exhibits a pretransitional increase while the viscosities along $\hat{\mathbf{y}}$ and $\hat{\mathbf{z}}$ (η_c and η_a, respectively) do not (see Fig. 4). By applying linear-response theory McMillan[26] found that within mean-field theory η_b should diverge as τ/ξ. If we use dynamical scaling, then τ is proportional to $\xi^{3/2}$ so η_b is proportional to $\xi^{1/2}$. Similar results were found by Janig and Brochard.[27]

In this section, we will examine how, within mean-field theory, the structure factor $S(\mathbf{q})$ behaves as we go to large Deborah numbers; that is, we will extend McMillan's theory beyond linear response. Use of mean-field theory is in part justified by the result of Onuki and Kawasaki[9] that for nonzero Deborah number we should expect mean-field critical behavior (the N–Sm-A phase boundary under shear flow is, however, still expected to deviate from mean-field theory). As was emphasized in the Introduction, large changes in $S(\mathbf{q})$ will change the macroscopic properties of a fluid and in particular the equation of motion of the director. The results of this section will thus serve as input for a discussion of the macroscopic properties in the following section.

The free energy associated with smectic fluctuations in the nematic phase is

$$F=\tfrac{1}{2}\int d^3r[\,A|\psi|^2+C_{\parallel}|(\hat{\mathbf{n}}\cdot\nabla-iq_0)\psi|^2 +C_{\perp}|(\hat{\mathbf{n}}\times\nabla)\psi|^2]\ . \tag{3.1}$$

The complex order parameter ψ describes a density wave associated with a fluctuation cluster. In the nematic phase ψ must be zero on average so $A>0$. We will assume that A is proportional to $T-T_{N\text{-Sm-}A}$. The second and third terms in F are the energy costs associated with spatial variations of the order parameter. The second term is the cost of variation along $\hat{\mathbf{n}}$, the third of variation perpendicular to $\hat{\mathbf{n}}$. Assuming we have a fluctuation cluster, Eq. (3.1) predicts that the cluster with the lowest cost in energy has a spatial variation proportional to $e^{iq_0(\mathbf{r}\cdot\hat{\mathbf{n}})}$, as should be expected for a density wave along $\hat{\mathbf{n}}$ of wave vector q_0. The density modulation associated with the cluster is

$$\rho(\mathbf{r})=\rho_0[1+\mathrm{Re}(\psi)]\ . \tag{3.2}$$

The correlation lengths parallel and perpendicular to $\hat{\mathbf{n}}$ are $\xi_{\parallel}=(C_{\parallel}/A)^{1/2}$ and $\xi_{\perp}=(C_{\perp}/A)^{1/2}$, respectively, so both $\xi_{\parallel}$ and $\xi_{\perp}$ diverge as $(T-T_{N\text{-Sm-}A})^{-1/2}$ within Landau theory. We are assuming here that the nematic director is spatially uniform.

In the absence of shear flow ψ tries to minimize F by going to zero, while thermal fluctuations push it away from $\psi=0$. Shear flow will exert an additional force on ψ. The complete equation of motion is the time-dependent Ginzburg-Landau equation in the presence of flow:[26]

$$\gamma_3\left[\frac{\partial\psi}{\partial t}+\mathbf{v}\cdot\nabla\psi\right]=-\frac{\delta F}{\delta\psi^*}+h(\mathbf{r},t)\ . \tag{3.3}$$

By neglecting spatial variations of ψ in Eq. (3.3), it follows that $\tau=\gamma_3/A$ is the order-parameter relaxation time (in the absence of flow). Equation (3.3) assumes that order-parameter fluctuations relax dissipatively towards equilibrium. The actual relaxation of a fluctuation cluster is by diffusion of molecules across smectic layers so γ_3 is of the order of the liquid viscosity. The flow field $\mathbf{v}$ is assumed to be that of simple shear:

$$\mathbf{v}=\dot{\gamma}y\hat{\mathbf{x}} \tag{3.4}$$

as in Sec. II. The Gaussian random variable $h(\mathbf{r},t)$ describes the coupling to ψ to thermal noise. Its correlation function is determined by the fluctuation-dissipation theorem:

$$\langle h(\mathbf{r},t)h(0,0)\rangle=2\gamma_3k_BT\delta(\mathbf{r})\delta(t)\ . \tag{3.5}$$

By using Eqs. (3.1) and (3.4), the equation of motion becomes

$$\gamma_3\left[\frac{\partial\psi}{\partial t}+\dot{\gamma}y\frac{\partial\psi}{\partial x}\right]=-[\,A\psi+C_{\parallel}(\hat{\mathbf{n}}\cdot\nabla-iq_0)^2\psi +C_{\perp}(\hat{\mathbf{n}}\times\nabla)^2\psi]+h(\mathbf{r},t)\ . \tag{3.6}$$

After applying the Fourier transform

$$\psi(\mathbf{r})=\int d^3\mathbf{q}\frac{1}{(2\pi)^{3/2}}\psi_{\mathbf{q}}e^{i\mathbf{q}\cdot\mathbf{r}}\ , \tag{3.7}$$

the equation of motion in momentum space turns into

$$\frac{\partial\psi_{\mathbf{q}}}{\partial t}-\dot{\gamma}q_x\frac{\partial\psi_{\mathbf{q}}}{\partial q_y}=-\Gamma_0(\mathbf{q})\psi_{\mathbf{q}}+h_{\mathbf{q}}(t)/\gamma_3\ . \tag{3.8}$$

The function

$$\Gamma_0(\mathbf{q})=\frac{A+C_{\parallel}(\hat{\mathbf{n}}\cdot\mathbf{q}-q_0)^2+C_{\perp}(\hat{\mathbf{n}}\times\mathbf{q})^2}{\gamma_3} \tag{3.9}$$

is the equilibrium (wave-vector-dependent) order-parameter decay rate and is proportional to $S_0^{-1}(\mathbf{q})$, the structure factor in the absence of flow. For $\dot{\gamma}=0$ the solution of Eq. (3.8), $\psi_{\mathbf{q}}^0$ is straightforward:

$$\psi_{\mathbf{q}}^0(t)=\int_{-\infty}^{t}dt'\exp[-(t-t')\Gamma_0(\mathbf{q})]h_{\mathbf{q}}(t')/\gamma_3\ . \tag{3.10}$$

The mean square of $\psi_{\mathbf{q}}^0$ is

$$\langle|\psi_{\mathbf{q}}^0(t)|^2\rangle=\int_{-\infty}^{t}dt'\int_{-\infty}^{t'}dt''\exp[-(2t-t'-t'')\Gamma_0(\mathbf{q})]\times\langle h_{\mathbf{q}}^*(t')h_{\mathbf{q}}(t'')\rangle/\gamma_3^2\ . \quad (3.11)$$

In the $t\to\infty$ limit, $\langle|\psi_{\mathbf{q}}^0(t)|^2\rangle$ should be proportional to the equilibrium density correlation function $\langle|\rho_{\mathbf{q}}|^2\rangle$ which in turn is just $S_0(\mathbf{q})$. From the equipartition theorem and Eq. (3.1), we have that

$$\langle|\psi_{\mathbf{q}}|^2\rangle_{\rm eq}=\left[\frac{1}{2\pi}\right]^3\frac{Vk_BT}{\gamma_3\Gamma_0(\mathbf{q})}\ . \quad (3.12)$$

(Here, the volume element V arises due to the usual substitution $\int d^3\mathbf{q}\to[(2\pi)^3/V]\sum_{\mathbf{q}}$. For simplicity, we shall set V equal to unity.) This is consistent with the fluctuation-dissipation relation of Eq. (3.5) which when inserted in Eq. (3.11) gives for zero flow

$$\Gamma_0(\mathbf{q})S_0(\mathbf{q})=\left[\frac{1}{2\pi}\right]^3k_BT/\gamma_3 \quad (3.13)$$

in agreement with Eq. (3.12). In Eq. (3.13) we have set the nematic density $\rho_0=1$, so that $S_0(\mathbf{q})\equiv\langle|\rho(\mathbf{q})|^2\rangle=\langle|\psi_{\mathbf{q}}|^2\rangle_{\rm eq}=\langle|\psi_{\mathbf{q}}^0(\infty)|^2\rangle$.

Now, we turn on the flow. The solution of Eq. (3.8) is then given by an *operator* equation:

$$\psi_{\mathbf{q}}(t)=\int_{-\infty}^{t}dt'\exp\left[-(t-t')\left[\Gamma_0(\mathbf{q})-\dot\gamma q_x\frac{\partial}{\partial q_y}\right]\right]\times h_{\mathbf{q}}(t')/\gamma_3\ . \quad (3.14)$$

Although this is not obvious, it can be checked that in computing $S(\mathbf{q})$ we may simply treat the operator $\partial/\partial q_y$ as if it was an ordinary number. Repeating the calculation which led to Eq. (3.13) then gives a partial differential equation for $S(\mathbf{q})$:

$$\left[\Gamma_0(\mathbf{q})-\dot\gamma q_x\frac{\partial}{\partial q_y}\right]S(\mathbf{q})=k_BT/\gamma_3\ . \quad (3.15)$$

The differential equation

$$\frac{df}{dx}+\alpha(x)f(x)=1 \quad (3.16)$$

has, for an arbitrary function $\alpha(x)$, the particular solution

$$f(x)=\int_0^\infty dx'\exp\left[-\int_0^{x'}d\zeta\,\alpha(x-\zeta)\right] \quad (3.17)$$

if $\int_0^\infty d\zeta\,\alpha(x-\zeta)=\infty$. If we apply this to Eq. (3.15) then the corresponding solution is

$$S(\mathbf{q})=\left[\frac{1}{2\pi}\right]^3\frac{k_BT}{\gamma_3}\times\int_0^\infty dt\exp\left[-\int_0^t d\zeta\,\Gamma_0(q_x,q_y+\dot\gamma q_x\zeta,q_z)\right]\ . \quad (3.18)$$

Homogeneous solutions to Eq. (3.15) are not included because they would lead to $S(\mathbf{q})=\infty$ at $q_x=0$. Using the definitions of $\Gamma_0(\mathbf{q})$ then leads to our central result for $S(\mathbf{q})$:

$$S(\mathbf{q})=\left[\frac{1}{2\pi}\right]^3\frac{k_BT}{\gamma_3}\times\int_0^\infty dt\exp\{-[\Gamma_0(\mathbf{q})t+\alpha(\mathbf{q})t^2+\beta(\mathbf{q})t^3]\} \quad (3.19)$$

with

$$\alpha(\mathbf{q})=\dot\gamma q_x[C_\parallel n_y(\mathbf{q}\cdot\hat{\mathbf{n}}-q_0)+C_\perp(-n_y\mathbf{q}\cdot\hat{\mathbf{n}}+q_y)]/\gamma_3\ , \quad (3.20a)$$

$$\beta(\mathbf{q})=\tfrac{1}{3}\dot\gamma^2q_x^2[C_\parallel n_y^2+C_\perp(n_x^2+n_z^2)]/\gamma_3\ . \quad (3.20b)$$

The structure factor assumes two different limiting forms depending on whether we are in the low- or high-Deborah-number regime. We first treat the low-shear-rate regime.

A. Small Deborah numbers

For $\dot\gamma\tau<1$, we can expand the exponential in Eq. (3.19) in powers of α and β. The validity condition for such an expansion is that $\Gamma_0^3\gg\beta$ and $\Gamma_0^2\gg\alpha$. The condition $\Gamma_0^3\gg\beta$ reduces to $\dot\gamma\tau q_x\xi\ll1$ with $\xi=[\xi_\parallel^2n_y^2+\xi_\perp^2(n_x^2+n_z^2)]^{1/2}$ and $\mathbf{q}$ close to $q_0\hat{\mathbf{n}}$. The condition $\Gamma_0^2\ll\alpha$ leads to a similar condition. To second order in $\dot\gamma\tau q_x\xi$,

$$S(\mathbf{q})=\left[\frac{1}{2\pi}\right]^3\frac{k_BT}{\gamma_3}\left[\frac{1}{\Gamma_0(\mathbf{q})}-\frac{2\alpha(\mathbf{q})}{\Gamma_0(\mathbf{q})^3}-\frac{6\beta(\mathbf{q})}{\Gamma_0(\mathbf{q})^4}+\frac{8\alpha^2(\mathbf{q})}{\Gamma_0(\mathbf{q})^5}+\cdots\right]\ . \quad (3.21)$$

Note that since

$$\alpha(\mathbf{q})=\tfrac{1}{2}\dot\gamma q_x\frac{\partial\Gamma_0}{\partial q_y} \quad (3.22)$$

we can include the first-order correction in Eq. (3.21) as

$$S(\mathbf{q})=\left[\frac{1}{2\pi}\right]^3\frac{k_BT}{\gamma_3}\Gamma_0^{-1}(q_x,q_y+\dot\gamma\tau(\mathbf{q})q_x,q_z)+0((\dot\gamma\tau)^2)+\cdots \quad (3.23)$$

with

$$\tau(\mathbf{q})\equiv\Gamma_0^{-1}(\mathbf{q}) \quad (3.24)$$

the equilibrium $\mathbf{q}$-independent order-parameter relaxation time. Note that $\tau(\mathbf{q}=\hat{\mathbf{n}}q_0)=\tau$. This result is the same as Eq. (2.6) if one replaces τ by $\tau(\mathbf{q})$. For $\mathbf{q}$ close to $\hat{\mathbf{n}}q_0$ this replacement is not a very important effect. The difference is important for large $|\mathbf{q}-q_0\hat{\mathbf{n}}|$ and is discussed in the following section.

One may readily verify from Eq. (3.23), that while for $\hat{\mathbf{n}}=\hat{\mathbf{z}}$ or $\hat{\mathbf{n}}=\hat{\mathbf{y}}$, $S(\mathbf{q})$ peaks at $(0,0,q_0)$ or $(0,q_0,0)$, respectively, for $\hat{\mathbf{n}}=\hat{\mathbf{x}}$ the peak in $S(\mathbf{q})$ is at $\mathbf{q}\simeq q_0(1,-\dot\gamma\tau,0)$, implying a finite tilt of the layer normal with $\hat{\mathbf{n}}$ (as we

found earlier in our geometrical model of Sec. II).

It is interesting to ask about the relaxation rate for order-parameter fluctuations under shear flow. At equilibrium the order-parameter relaxation rate is given by $\Gamma_0(\mathbf{q})$. Thus one expects that for $\dot\gamma\tau \ll 1$, $\Gamma_0(\mathbf{q},\dot\gamma) \simeq \Gamma_0(q_x, q_y + \dot\gamma\tau q_x, q_z)$ so that

$$\Gamma_0(\mathbf{q},\dot\gamma) \simeq \Gamma_0(\mathbf{q}) + 2(\dot\gamma\tau)\frac{C_\perp}{\gamma_3} q_x q_y + (\dot\gamma\tau)^2 \frac{C_\perp}{\gamma_3} q_x^2 . \tag{3.25}$$

Therefore, to lowest order in $(\dot\gamma\tau)$, the lifetime of order-parameter fluctuation modes normal to the shear plane, i.e., with $q_x = q_y = 0$, is unaffected by shear, whereas fluctuation modes with wave vector along the flow direction (i.e., with $q_x \neq 0$) are strongly affected and decay more rapidly. This is consistent with the simple geometrical picture of Sec. II where we found that fluctuation clusters with the director aligned along the flow direction lead to a tilting of the smectic layers [Eq. (2.11)] which tends to reduce the layer spacing and is energetically costly. A smectic fluctuation with this orientation will therefore dissipate more rapidly.

Before proceeding to high Deborah numbers, we first calculate the overall magnitude of the smectic fluctuations for $\dot\gamma \neq 0$ using $\langle |\psi|^2 \rangle = \int d^3q S(\mathbf{q})$. The result will be used later in our calculation of the nematic–smectic-A transition temperature and of the nematic elastic constants and viscosities under shear flow. From Eq. (3.23) we find that (Appendix B)

$$\langle |\psi|^2 \rangle \simeq \langle |\psi|^2 \rangle_{\dot\gamma=0} - \frac{1}{192\pi}\frac{k_B T}{C_\perp \xi_\parallel}(\dot\gamma\tau)^2 + \cdots + O(\dot\gamma\tau)^4 \quad (\dot\gamma\tau \to 0) . \tag{3.26}$$

Since the second term is negative definite, it follows that fluctuations are suppressed by shear flow. The same trend was noted by Onuki and Kawasaki in their study of binary fluids under shear flow.

B. Large Deborah numbers

For larger Deborah numbers, $\dot\gamma\tau > 1$, we have three different regimes in $\mathbf{q}$ space. We will discuss these for the case $\hat{\mathbf{n}} = \hat{\mathbf{z}}$, which is most relevant for experiment.[12] In that case we have

$$\begin{aligned} \alpha &= \dot\gamma C_\perp q_x q_y / \gamma_3 , \\ \beta &= \tfrac{1}{3}\dot\gamma^2 C_\perp q_x^2 / \gamma_3 , \\ \Gamma_0 &= [A + C_\parallel (q_\parallel - q_0)^2 + C_\perp q_\perp^2]/\gamma_3 . \end{aligned} \tag{3.27}$$

We first look for the region in $\mathbf{q}$ space where the perturbation result for $S(\mathbf{q})$ [Eq. (3.21)] still applies. As can be seen from Eq. (3.23), the validity condition is $\dot\gamma\tau(\mathbf{q}) q_x \ll q_y$. For $q_y\xi_\perp$ comparable to 1, this means that the small parameter of the perturbation series is $\dot\gamma\tau(\mathbf{q}) q_x \xi_\perp$. This parameter is small when $q_x \to 0$. If $q_y \ll 1/\xi_\perp$, so that $\dot\gamma\tau q_x > q_y$, the perturbation result is still valid as long as $q_x < 1/(\dot\gamma\tau)\xi_\perp$. (This is readily seen if one sets $q_y = 0$, but still demands that $\Gamma_0^3 > \beta$.) We refer to this small q_x limit as regime I. In fact, it follows immediately from Eqs. (3.19) and (3.20) that for $q_x = 0$, $S(\mathbf{q})$ is *independent* of the shear rate $\dot\gamma$ since $\alpha = \beta = 0$. This means that $S(0, q_y, q_z) = (1/2\pi)^3 k_B T/\Gamma_0(0, q_y, q_z)\gamma_3$.

For large $\mathbf{q}$, $\tau(\mathbf{q})$ goes to zero and perturbation theory becomes valid once again. This q range, which we call regime III (see below), is obtained by requiring that $\Gamma_0^2 > \alpha$ and $\Gamma_0^3 > \beta$ for large $|\mathbf{q} - q_0\hat{\mathbf{z}}|$. Thus the two regimes where the perturbation result of Eq. (3.23) is valid can be summarized:

$$S(\mathbf{q}) \approx \left[\frac{1}{2\pi}\right]^3 k_B T \Gamma_0^{-1}(q_x, q_y + \dot\gamma\tau(\mathbf{q}) q_x, q_z) + O((\dot\gamma\tau)^2) \begin{cases} |q_x| \lesssim (\dot\gamma\tau\xi_\perp)^{-1} & \text{(regime I)} \\ [q] \gtrsim \left[(\tfrac{1}{3})^{1/3} \left[\dfrac{\gamma_3 \dot\gamma q_x}{C_\perp} \right]^{2/3} - \xi_\perp^{-2} \right]^{1/2} & \text{(regime III)} , \end{cases} \tag{3.28}$$

where $[q] \equiv [q_\perp^2 + (C_\parallel/C_\perp)(q_\parallel - q_0)^2]^{1/2}$ is a rescaled $|\mathbf{q}|$ (with $C_\parallel > C_\perp$). For a typical value of q_x on the order of $1/\xi_\perp$, the boundary of regime III is $[q] \gtrsim (1/\xi_\perp)[(\dot\gamma\tau/\sqrt{3})^{2/3} - 1]^{1/2}$. Perturbation theory thus remains valid in a thin sheet around the $q_x = 0$ plane and outside an anisotropic regime in $\mathbf{q}$ space defined by Eq. (3.28).

The most interesting case is what happens inside regime II where both inequalities in Eq. (3.28) are violated. Now, the integral in Eq. (3.19) is dominated by the term $\beta(q)t^3$ in the exponent and $S(\mathbf{q})$ is highly distorted. For large β, one finds that (Appendix A)

$$S(\mathbf{q}) \approx \left[\frac{1}{2\pi}\right]^3 \frac{k_B T}{\gamma_3} \left[\frac{\Gamma(\frac{1}{3})}{3\beta^{1/3}} - \frac{\alpha}{3\beta} - \frac{\Gamma(\frac{2}{3})}{3\beta^{2/3}} \left[\Gamma_0 - \frac{\alpha^2}{3\beta} \right] + \frac{\Gamma(\frac{1}{3})}{9\beta^{4/3}} \alpha\Gamma_0 \right] + O\left[\frac{1}{\dot\gamma^2}\right] \quad \text{(regime II)} . \tag{3.29}$$

Here $\Gamma(x)$ is the gamma function and the $\mathbf{q}$-dependent functions Γ_0, α, and β were defined earlier. Equation (3.29) is actually an expansion in $1/(\dot\gamma\tau)^{1/3}$ which converges very slowly.

In the limit $\dot\gamma\tau \to \infty$, $S(\mathbf{q})$ thus has a *power-law dependence* on q_x: $S(\mathbf{q}) \simeq (1/\dot\gamma^2 q_x^2)^{1/3}$ while it is independent of q_y and q_z. We thus predict for $\dot\gamma\tau \gg 1$, *sheets* of scattering parallel to the $q_x = 0$ plane. Sheets of scattering are indicative of one-dimensional correlations. The fluctuation clusters thus must consist of very long strings lined up along the flow direction as we already argued in Sec. II. In real space, the density-density correlation function drops off as a power law:

$$\langle \rho(\mathbf{x})\rho(0) \rangle \propto \left[\frac{1}{x}\right]^{1/3} \delta(y)\delta(z) \tag{3.30}$$

for $|x| < \dot\gamma\tau\xi_\perp$ and $\dot\gamma\tau \gg 1$.

To physically understand the boundaries of regime II

where $S(\mathbf{q})$ is highly distorted we recall the dynamical scaling argument presented in Sec. I. From this scaling law, we expect that the shear rate $\dot{\gamma}$ determines a threshold q_s [$\propto \dot{\gamma}^{1/z}$, Eq. (1.4b)] such that for $q < q_s$ we expect $S(\mathbf{q})$ to be distorted, but for $q > q_s$, the order-parameter fluctuations relax so fast that shear has little effect. We now show that q_s in fact separates the distorted regime II from the undistorted regime III.

From Sec. I [see Eq. (1.4a)], we found that q_s is defined through the condition $\omega(q_s)=\dot{\gamma}$, where $\omega(q)$ is the order-parameter relaxation rate $\Gamma_0(\mathbf{q})$ given by Eq. (3.9). Therefore the condition $\omega(q_s)=\dot{\gamma}$ gives

$$[q]_s \equiv \left[q_{\perp s}^2 + \frac{C_\parallel}{C_\perp}(q_{\parallel s}-q_0)^2 \right]^{1/2} \cong \frac{1}{\xi_\perp}(\dot{\gamma}\tau - 1)^{1/2} , \quad (3.31)$$

which is meaningful only for $\dot{\gamma}\tau > 1$. When q_x is of order $1/\xi_\perp$ and $\dot{\gamma}\tau \gtrsim 1$, the boundary in q space between regimes II and III defined in Eq. (3.28) agrees qualitatively with the dynamic scaling result of Eq. (3.31).

We point out here that Eq. (3.31) [or Eq. (3.28)] predicts that there is a threshold Deborah number $(\dot{\gamma}\tau)_s$ such that for $(\dot{\gamma}\tau) > (\dot{\gamma}\tau)_s \approx 0(1)$ the cutoff wave vector $[q]_s$ grows rapidly. That is, the onset of distortion in $S(\mathbf{q})$ occurs rapidly over a small range of $(\dot{\gamma}\tau)$. This behavior is a direct consequence of the *nonconserved* nature of the smectic-A order parameter for this transition as discussed in the Introduction. For a conserved order parameter (e.g., binary fluids), the growth in $[q]_s$ starts immediately for $\dot{\gamma}\tau \gtrsim 0$.

If we consider $\hat{\mathbf{n}}$ oriented along the flow direction ($\hat{\mathbf{n}}=\hat{\mathbf{x}}$), then the boundary between regime II [where $S(\mathbf{q})$ is distorted] and regime III [where $S(\mathbf{q})$ is essentially unaffected] is given by

$$[q]_s \simeq \left[(\tfrac{1}{3})^{1/3} \left(\frac{\gamma_3 \dot{\gamma} q_0}{C_\perp} \right)^{2/3} - \xi_\perp^{-2} \right]^{1/2}$$
$$= \frac{1}{\xi_\perp}[(\tfrac{1}{3})^{1/3}(\dot{\gamma}\tau q_0 \xi_\perp)^{2/3} - 1]^{1/2} . \quad (3.32)$$

The rapid onset of distortion where $[q]_s$ grows then occurs around $\dot{\gamma}\tau q_0 \xi_\perp \gtrsim 1$. Since normally $q_0\xi_\perp \gg 1$, $S(\mathbf{q})$ with $\hat{\mathbf{n}} \| \mathbf{v}$ is suppressed significantly earlier than $S(\mathbf{q})$ with $\hat{\mathbf{n}} \perp \mathbf{v}$ as the temperature is reduced in approaching the nematic to smectic-A phase transition.

To understand the boundary between regimes I and II, we recall our geometrical argument where we found that the effective correlation length along the flow direction $\xi^+ \simeq \dot{\gamma}\tau\xi$ for $\dot{\gamma}\tau \gg 1$. Furthermore, $S(0,q_y,q_z)$ is unchanged by shear flow. For length scales q_x^{-1} large compared to the correlation lengths this should remain the case. Consequently, $|q_x| = 1/\xi^+$ should mark the boundary where distortion starts.

IV. CRITICAL NEMATIC HYDRODYNAMICS

In the preceding sections, we discussed the effect of shear flow on the microscopic structure factor $S(\mathbf{q})$. We will now use the results to investigate the effect of shear flow on the macroscopic properties of a nematic liquid crystal close to the transition temperature. Shear flow must change the macroscopic behavior since for large Deborah numbers the fluctuation clusters, which influence both the static and dynamic properties of the nematic liquid crystal, are deformed and suppressed. A smectic cannot support, twist, or bend in the director because it changes the interlayer spacing. It follows that the corresponding stiffness constants K_2 and K_3 of the nematic liquid crystal must diverge at the transition temperature as the size of the fluctuation clusters diverges.[20,28,29] In the same way, the viscosity of the b orientation of the nematic phase, η_b, must diverge at $T_{N\text{-Sm-}A}$ since shear flow would alter the layer spacing of clusters which have their layer normal along the flow direction.[26,27,30,31]

The presence of the sheared fluctuation clusters leads to a fluctuation torque which tries to orient $\hat{\mathbf{n}}$ in a plane perpendicular to the flow direction to avoid changes in the interlayer spacing. This new torque is analogous to the "normal forces" encountered in the rheology of polymeric fluids. Shear flow also reduces the magnitude of the correlation volume, as we saw in the preceding section. This will be shown to lead to a reduction under shear flow of K_2, K_3, and η_b analogous to the shear thinning of polymeric fluids.

A. Nematic hydrodynamics

The classical equation of motion for the nematic director is given by the Ericksen-Leslie[21,22] equation of nematic hydrodynamics:

$$\boldsymbol{\Gamma}_f + \boldsymbol{\Gamma}_v = \mathbf{0} , \quad (4.1)$$

where

$$\boldsymbol{\Gamma}_f = \hat{\mathbf{n}} \times \mathbf{h} \quad (4.2)$$

is the torque on the director due to the molecular field[11] $\mathbf{h} = -\delta F / \delta \hat{\mathbf{n}}$, and where $\boldsymbol{\Gamma}_v$ is the viscous torque. The molecular field is due to the torques on the director created by the fluctuation clusters, which we refer to as the fluctuation torque, and by a splay, bend, or twist in the director field; that is, the elastic torque. We consider the fluctuation torque in the following section.

The viscous torque (per unit volume) exerted on the nematic director by an imposed flow field $\mathbf{v}$ is

$$\boldsymbol{\Gamma}_v = -\hat{\mathbf{n}} \times (\gamma_1 \mathbf{N} + \gamma_2 \overleftrightarrow{\mathbf{A}} \cdot \hat{\mathbf{n}}) \quad (4.3)$$

with $\mathbf{N}$ the total rate of change of $\hat{\mathbf{n}}$:

$$\mathbf{N} = \frac{\partial \hat{\mathbf{n}}}{\partial t} - \boldsymbol{\omega} \times \hat{\mathbf{n}} \quad (4.4)$$

and with $\boldsymbol{\omega} = \frac{1}{2}\nabla \times \mathbf{v}$ the vorticity. The symmetrized shear rate tensor $\overleftrightarrow{\mathbf{A}}$ is

$$A_{ij} = \frac{1}{2}\left(\frac{\partial v_i}{\partial x_j} + \frac{\partial v_j}{\partial x_i} \right) . \quad (4.5)$$

γ_1 and γ_2 are viscosity coefficients which control nematic flow alignment and are related to the Leslie α parameters by

$$\alpha_2=\tfrac{1}{2}(\gamma_2-\gamma_1)\ , \tag{4.6a}$$

$$\alpha_3=\tfrac{1}{2}(\gamma_1+\gamma_2)\ . \tag{4.6b}$$

If $\mathbf{v}=\dot\gamma y\hat{\mathbf{x}}$ then Eq. (4.1) becomes

$$\hat{\mathbf{n}}\times\left[\gamma_1\frac{\partial\hat{\mathbf{n}}}{\partial t}+\dot\gamma(\alpha_2 n_y,\alpha_3 n_x,0)-\mathbf{h}\right]=\mathbf{0}\ . \tag{4.7}$$

We see from Eq. (4.7) that α_3 is proportional to the Miesowicz viscosity η_b measured with $\hat{\mathbf{n}}=n_x\hat{\mathbf{x}}$ (see Appendix C).

In Appendix C we show that Eq. (4.7) predicts that for $\mathbf{h}=\mathbf{0}$, the $\hat{\mathbf{n}}=\hat{\mathbf{z}}$ orientation is *unstable* if $\alpha_2\alpha_3>0$ and *marginally stable* if $\alpha_2\alpha_3<0$. Since $\alpha_2<0$,[31] we expect the $\hat{\mathbf{n}}=\hat{\mathbf{z}}$ orientation (the a orientation) to be marginally stable if $\alpha_3>0$. When $\alpha_3<0$, we show in Appendix C that the a orientation is unstable and that there is a stable solution with the director in the x-y shear plane with $\hat{\mathbf{n}}$ pointing almost along the flow direction (the b orientation).

The elastic torque in Eq. (4.7) is due to a spatial variation of $\hat{\mathbf{n}}$. In the one constant approximation $K=K_1=K_2=K_3$,[11]

$$\mathbf{h}=K\nabla^2\hat{\mathbf{n}}\ . \tag{4.8}$$

B. Fluctuation torque

Close to $T_{N\text{-Sm-}A}$, a new torque appears associated with the above-mentioned flow deformation of the fluctuation clusters.

From Eq. (3.1) if follows that for a *uniform* director field the average molecular field $\mathbf{h}\equiv-\int d^3\mathbf{r}\,\delta F/\delta\mathbf{n}$ is given by

$$\mathbf{h}=-2\int d^3\mathbf{q}[C_\parallel\mathbf{q}(\hat{\mathbf{n}}\cdot\mathbf{q}-q_0)+C_\perp(\hat{\mathbf{n}}q^2-\mathbf{q}(\hat{\mathbf{n}}\cdot\mathbf{q}))]|\psi_{\mathbf{q}}|^2\ . \tag{4.9}$$

This integral is dominated by the region in $\mathbf{q}$ space around $\mathbf{q}=\hat{\mathbf{n}}q_0$. This means that the term proportional to $C_\parallel$ in Eq. (4.9) can be dropped as it has a zero at $\mathbf{q}=\hat{\mathbf{n}}q_0$. Furthermore, since the torque on the director is given by $\hat{\mathbf{n}}\times\mathbf{h}$, we also may drop terms in $\mathbf{h}$ proportional to $\hat{\mathbf{n}}$. The result is

$$\mathbf{h}=2C_\perp\int d^3q\,\mathbf{q}(\hat{\mathbf{n}}\cdot\mathbf{q})|\psi_{\mathbf{q}}|^2\ . \tag{4.10}$$

In the spirit of mean-field theory, we now replace $|\psi_{\mathbf{q}}|^2$ by its expectation value $S(\mathbf{q})$ so

$$\mathbf{h}=2C_\perp\int d^3q\,\mathbf{q}(\hat{\mathbf{n}}\cdot\mathbf{q})S(\mathbf{q}) \tag{4.11}$$

is the first moment of $S(\mathbf{q})$ under shear flow (with $\mathbf{q}\approx\hat{\mathbf{n}}q_0$). In Secs. I and II we discussed the effect of shear flow on $S(\mathbf{q})$ so we are now in a position to compute this fluctuation torque.

1. *Fluctuation torque: The a orientation*

We start by considering the a orientation, i.e., with $\hat{\mathbf{n}}$ close to the $\hat{\mathbf{z}}$ direction.

The value of $\mathbf{h}$ for this orientation is calculated in Appendix B. For low Deborah numbers $\dot\gamma\tau<1$, we find

$$\mathbf{h}\simeq-\frac{1}{8\pi}(\dot\gamma\tau)\frac{q_0^2}{\xi_\parallel}k_BT\delta n_x\hat{\mathbf{y}}-\frac{1}{96\pi}(\dot\gamma\tau)^2\frac{q_0^2}{\xi_\parallel}k_BT\delta n_x\hat{\mathbf{x}}+\frac{9}{640\pi}(\dot\gamma\tau)^3\frac{q_0^2}{\xi_\parallel}k_BT\delta n_x\hat{\mathbf{y}}+O(\dot\gamma\tau)^4\ . \tag{4.12}$$

If we include Eq. (4.12) in Eq. (4.7), we find

$$\gamma_1^R\partial_t\delta\hat{\mathbf{n}}+\left[\dot\gamma\alpha_2\delta n_y+\frac{\gamma_1^R}{\tau_N}\delta n_x,\dot\gamma\alpha_3^R\delta n_x\right]=K\nabla^2\delta\hat{\mathbf{n}}\ . \tag{4.13}$$

In Eq. (4.13)

$$\alpha_3^R=\alpha_3+\frac{1}{8\pi}\frac{q_0^2}{\xi_\parallel}k_BT[1-\tfrac{9}{80}(\dot\gamma\tau)^2+\cdots] \tag{4.14a}$$

and

$$\tau_N^{-1}=\frac{1}{96\pi}\frac{(\dot\gamma\tau)^2}{\gamma_1\xi_\parallel}q_0^2k_BT \tag{4.14b}$$

and

$$\gamma_1^R=\alpha_3^R-\alpha_2\ . \tag{4.14c}$$

The origin of the renormalization of γ_1 is discussed in the following section. Looking for solutions to Eq. (4.13) proportional to $e^{i[\mathbf{q}\cdot\mathbf{r}+\omega(\mathbf{q})t]}$ we find, for the mode spectrum $\omega(\mathbf{q})$,

$$\omega^{\pm}(\mathbf{q})=i\left[\frac{Kq^2}{\gamma_1^R}+\frac{1}{2\tau_N}\right]\pm\left[\omega_0^2-\left[\frac{1}{2\tau_N}\right]^2\right]^{1/2}\ , \tag{4.15a}$$

where

$$\omega_0=\frac{\dot\gamma}{\gamma_1^R}(-\alpha_2\alpha_3^R)^{1/2}\ . \tag{4.15b}$$

(i) Uniform precession. To discuss this mode spectrum, we first restrict ourselves to $\mathbf{q}=\mathbf{0}$. We can then rewrite Eq. (4.13) as a single equation for $\delta n_x(t)$:

$$\partial_t^2\delta n_x+\tau_N^{-1}\partial_t\delta n_x+\omega_0^2\delta n_x=0\ . \tag{4.16}$$

This is the equation of motion of a damped harmonic oscillator provided ω_0 is real, i.e., provided $\alpha_2\alpha_3^R<0$. If $\alpha_2\alpha_3^R>0$ then δn_x increases exponentially in time. The damping rate of the oscillator is τ_N^{-1}. If $(2\tau_N)^{-1}<\omega_0$, the oscillator is underdamped while if $(2\tau_N)^{-1}>\omega_0$ it is overdamped. The oscillation corresponds to a precession of the director around the $\hat{\mathbf{z}}$ axis. The $\pm$ sign of $\omega^{\pm}(\mathbf{q})$ corresponds to the helicity of the precession. If $\alpha_2\alpha_3^R<0$, the angle of the precession cone decays to zero while if $\alpha_2\alpha_3^R>0$, the angle increases in time.

We thus conclude that for $\dot\gamma\neq0$, the $\hat{\mathbf{z}}$ orientation is *stable* if $\alpha_2\alpha_3^R<0$ and *unstable* if $\alpha_2\alpha_3^R>0$. The point $\alpha_3^R=0$ marks the textural instability for $\dot\gamma\neq0$. It is clear from Eq. (4.13) that we can consider α_3^R as a renormalized Leslie parameter. If we follow the temperature dependence of α_3^R on approaching $T_{N\text{-Sm-}A}$, then for $\dot\gamma=0$, α_3^R

diverges at $T_{N\text{-Sm-}A}$ as $\tau/\xi_\parallel$. Since, in dynamical scaling, τ is proportional to $\xi^{3/2}$, α_3^R must be proportional to $\xi^{1/2}$. Because $\alpha_3<0$, this result predicts a *sign change* in α_3 at a temperature T_t close to $T_{N\text{-Sm-}A}$. For $\dot\gamma\tau\ll 1$, $\alpha_3^R=0$ at T_t where, using Eq. (4.14a),

$$|\alpha_3|=\frac{1}{8\pi}q_0^2 k_B T_t \tau(T_t)/\xi_\parallel(T_t)\ . \tag{4.17}$$

This sign change of α_3^R appears to be documented in the experimental literature.[30,32] Typically, T_t is at a temperature where $t_t=(T_t-T_{N\text{-Sm-}A})/T_{N\text{-Sm-}A}\simeq 0.01$. As we saw, T_t must also mark the stability limit of the a orientation (i.e., the a orientation is stable for $T_{N\text{-Sm-}A}<T<T_t$).

Now consider the contribution of the term proportional to $(\dot\gamma\tau)^2$ in Eq. (4.14a) [which comes from the third-order $(\dot\gamma\tau)^3$ term of Eq. (4.12)]. This reduction of α_3^R with shear flow is an example of the shear-thinning effect mentioned in the Introduction. Equation (4.14a) shows that for $\dot\gamma\tau$ of order 1, the renormalization of α_3 is suppressed. Note that we need to go to rather large Deborah numbers ($\dot\gamma\tau\approx 3$) before the shear-thinning effect really becomes significant. Because of this shear thinning, the critical temperature of the textural instability is affected by shear flow. If we set $\alpha_3^R=0$ and use Eq. (4.14a) with $\dot\gamma\neq 0$, we find that T_t is reduced by an amount $\Delta T_t(\dot\gamma)$ given by

$$\Delta T_t(\dot\gamma)=-\tfrac{9}{80}(\dot\gamma\tau)^2\Big/\left|\frac{\partial}{\partial T}\ln(\tau/\xi_\parallel)\right|_{T=T_t}\ . \tag{4.18}$$

We now turn to the damping rate τ_N^{-1}. The appearance of this damping mechanism for the precession around the $\hat{\mathbf{z}}$ axis represents a violation of conventional nematic dynamics: unlike h_y we cannot adsorb h_x into a redefinition of the Leslie parameters. By analogy to the theory of polymeric fluids we will call the new term a "normal" torque. It had not been noted in previous studies[26,27] of the dynamics of nematic liquid crystals since those were restricted to the linear-response regime while $\tau_N^{-1}\propto(\dot\gamma\tau)^2$.

The effect of the new term is, as we saw, to stabilize the a orientation. For $(1/2\tau_N)^2>\omega_0^2$, the precession is suppressed since $\omega(\mathbf{q}=0)$ becomes purely imaginary. There is thus a threshold shear rate $\bar{\dot\gamma}$ when $1/2\tau_N=\omega_0$ beyond which there is only relaxation. Using Eqs. (4.14) and (4.15) we find that $\bar{\dot\gamma}$ is given by

$$\bar{\dot\gamma}\simeq\frac{24}{\tau}\left[\frac{(-\alpha_2)\alpha_3^R}{(\alpha_3^R-\alpha_3)^2}\right]^{1/2}\propto\frac{1}{\xi^{7/4}}\ . \tag{4.19}$$

Thus, since $\xi\sim(T-T_{N\text{-Sm-}A})^{-\nu}$, the temperature at which the director mode becomes overdamped scales with shear:

$$\Delta T=(T-T_{N\text{-Sm-}A})\sim\dot\gamma^{\,4/7\nu}\ . \tag{4.20}$$

(ii) Finite q modes. For $\dot\gamma=0$, the mode spectrum $\omega(\mathbf{q})=iKq^2/\gamma_1^R$ of the orientational fluctuations is purely imaginary and—as expected from Goldstone modes—gapless. A perturbation in $\hat{\mathbf{n}}(\mathbf{r})$ thus relaxes diffusively. For $0<\dot\gamma\ll\bar{\dot\gamma}$, the mode spectrum is

$$\omega^{\pm}(\mathbf{q})\simeq\pm\omega_0+i\left[\frac{1}{2\tau_N}+\frac{Kq^2}{\gamma_1^R}\right]\quad(\dot\gamma\ll\bar{\dot\gamma})\ . \tag{4.21}$$

The precession relaxes but the damping rate does not go to zero for $\mathbf{q}=0$. The two helicities have the same damping rates. For $\tau_N^{-1}\gg\dot\gamma\gg\bar{\dot\gamma}$, on the other hand, there is no more precession. The mode spectrum

$$\begin{aligned}\omega^+(\mathbf{q})&\simeq i\left[\frac{Kq^2}{\gamma_1^R}+\frac{1}{\tau_N}\right],\\ \omega^-(\mathbf{q})&\simeq i\left[\frac{Kq^2}{\gamma_1^R}+\omega_0^2\tau_N\right]\quad(\dot\gamma\gg\bar{\dot\gamma})\ .\end{aligned} \tag{4.22}$$

The two helicities now have different damping rates because of the symmetry-breaking effect of shear flow. The damping rate of ω^+ grows with $\dot\gamma$ as $\dot\gamma^2$ while ω^- has a $q=0$ damping rate $\omega_0^2\tau_N$ which is *independent* of $\dot\gamma$. Near $T_{N\text{-Sm-}A}$, $\omega_0^2\tau_N\propto(-\alpha_2)/\gamma_1^R\tau$ which vanishes at $T_{N\text{-Sm-}A}$. We thus conclude that near $T_{N\text{-Sm-}A}$ and for $\dot\gamma\gg\bar{\dot\gamma}$, we recover the original gapless mode for one of the two helicities while the remaining helicity is strongly damped. We now consider the fluctuation torque for large Deborah numbers.

For large Deborah numbers, we saw from Sec. III [Eq. (3.28)], that there are three different regions of momentum space for $S(\mathbf{q})$. The integral in Eq. (4.11) cannot be performed analytically. The dominant contribution at moderately large Deborah numbers is from region I with $|q_x|\lesssim(\dot\gamma\tau\xi_\perp)^{-1}$ since it contains the maximum of $S(\mathbf{q})$. The contribution of region I to the molecular field is of order (Appendix B)

$$\mathbf{h}^{\mathrm{I}}\simeq c_2\frac{q_0^2}{\xi_\parallel}k_BT\delta n_x\hat{\mathbf{y}}-c_3\left[\frac{1}{|\dot\gamma\tau|}\right]\frac{q_0^2}{\xi_\parallel}k_BT\delta n_x\hat{\mathbf{x}} \tag{4.23}$$

with c_2 and c_3 constants. The "one-dimensional" power-law regime II contributes terms to $\mathbf{h}$ of order $(1/\xi_\parallel\xi_\perp^2)k_BT(\dot\gamma\tau)^{2/3}$ which will become important at Deborah numbers of order $(\xi_\perp/d)^3$ with d the layer spacing. This, however, is far outside the experimentally accessible regime near $T_{N\text{-Sm-}A}$. If we compare Eq. (4.23) with Eq. (4.14a), then we see that the renormalization of α_3 is much smaller for large Deborah numbers than for small Deborah numbers:

$$\alpha_3^R-\alpha_3\approx\frac{q_0^2k_BT}{\xi_\parallel|\dot\gamma\tau|}\quad(\dot\gamma\tau\gg1)\ . \tag{4.24}$$

Shear flow has, for $\dot\gamma\tau\gg1$, destroyed the fluctuation clusters and, as a consequence, the renormalization of α_3. In essence, we are back in the regime of conventional nematic dynamics for very large Deborah numbers.

2. *Fluctuation torque: The b orientation*

We now turn to the b orientation with the director aligned along the flow direction. Let $\alpha_3^R(b)$ be the α_3 viscosity along the b direction. We start by noting that we should expect the shear-thinning effect to be considerably more pronounced for the b orientation. Recall that

distortions in $S(\mathbf{q})$ become noticeable if $\beta(\mathbf{q}) \gtrsim \Gamma_0^3(\mathbf{q})$. For $n_x = 1$, we see from Eqs. (3.9) and (3.20b) that distortions are expected for the b orientation if $\dot{\gamma}\tau(\mathbf{q}) q_0 \xi \gtrsim 1$ since $q_x \approx q_0$. Since $q_0\xi \gg 1$ near $T_{N\text{-Sm-}A}$, we apparently enter the regime of high shear rates much earlier than for the a orientation where we saw that $\dot{\gamma}\tau(\mathbf{q}) \gtrsim 1$ was the required condition. For $\dot{\gamma}\tau q_0 \xi \ll 1$, perturbation theory applies and

$$\alpha_3^R(b) \approx \alpha_3 + \frac{1}{8\pi}\frac{\tau}{\xi_\parallel} q_0^2 k_B T \quad (\dot{\gamma}\tau q_0 \xi \ll 1) \tag{4.25}$$

as before. In Appendix D we show that for $\dot{\gamma}\tau q_0 \xi \gg 1$

$$\alpha_3^R(b) \approx \alpha_3 + \frac{1}{6\pi^2}\frac{\tau}{\xi_\parallel} q_0^2 k_B T \left[\frac{\sqrt{3}}{\dot{\gamma}\tau q_0 \xi}\right]^{1/3}, \quad 1 \ll \dot{\gamma}\tau q_0 \xi \ll q_0 \xi \tag{4.26}$$

using the method discussed in the preceding subsection. The stability condition for the b orientation is $\alpha_3^R(b) < 0$. Assume that $T_{N\text{-Sm-}A} < T < T_t$ so $\alpha_3^R(b) > 0$ for $\dot{\gamma}\tau = 0$. According to Eq. (4.26), $\alpha_3^R(b) < 0$ for $\dot{\gamma}\tau q_0 \xi \gg 1$. The shear flow apparently *restabilizes* the b orientation. The critical shear rate $\dot{\gamma}_c$ marking the restabilization is given by $\alpha_3^R(b) = 0$ or

$$\dot{\gamma}_c \simeq \frac{\sqrt{3}}{q_0 \xi_\perp \tau}\left[-\frac{3\pi^2}{2}\frac{\alpha_3 \xi_\parallel}{\tau q_0^2 k_B T}\right]^{-3}. \tag{4.27}$$

We found previously that along the a orientation, α_3^R remains positive until $\dot{\gamma}\tau$ is considerably larger than 1 [Eq. (4.14a)]. Apparently, over a considerable range of Deborah numbers *both* the a and b orientations are stable. We will dub this effect "textural hysteresis." The dependence of the textural stability on shear rate is thus, for $T_{N\text{-Sm-}A} < T \lesssim T_t$ (i.e., where α_3^R is positive),

Deborah number	a orientation	b orientation
$\dot{\gamma}\tau \ll 1/q_0\xi$	Stable	Unstable
$\frac{1}{q_0\xi} \ll \dot{\gamma}\tau \ll 1$	Stable	Stable
$\dot{\gamma}\tau \gg 1$	Unstable	Stable

We have restricted ourselves to shear thinning in this section. The other signatures of non-Newtonian liquids are "normal-stress" effects. They are present as well in our case, as discussed in Appendix F.

C. Viscosity renormalization

In Sec. IV B we computed the molecular field $\mathbf{h}$ assuming $\hat{\mathbf{n}}$ to be independent of time. For $(\partial/\partial t)\hat{\mathbf{n}} \neq \mathbf{0}$, there are actually correction terms which produce the renormalization of the dynamic viscosity γ_1. To calculate these dynamic corrections we assume, for the moment, that we have a pure vortex flow, i.e., $\vec{\mathbf{A}}\cdot\hat{\mathbf{n}} = 0$. The equation of motion then reduces to

$$\hat{\mathbf{n}} \times \left[\gamma_1\left[\frac{\partial \hat{\mathbf{n}}}{\partial t} - \boldsymbol{\omega}\times\mathbf{n}\right] - \mathbf{h}\right] = \mathbf{0}\,. \tag{4.28}$$

For $\partial\hat{\mathbf{n}}/\partial t = \boldsymbol{\omega}\times\hat{\mathbf{n}}$, the term in large square brackets must vanish as it corresponds to rigid-body rotation. This means that $\mathbf{h}$ also must be a function of $\partial\mathbf{n}/\partial t - \boldsymbol{\omega}\times\hat{\mathbf{n}}$ for a pure vorticity. We can now find the dynamic corrections to $\mathbf{h}$ by computing $\mathbf{h}$ as a function of $\omega\times\hat{\mathbf{n}}$ for $\partial\hat{\mathbf{n}}/\partial t = 0$ and then everywhere replacing $\boldsymbol{\omega}\times\hat{\mathbf{n}}$ by $\boldsymbol{\omega}\times\hat{\mathbf{n}} - \partial\hat{\mathbf{n}}/\partial t$.

The calculation of $\mathbf{h}$ for a pure vorticity, $\mathbf{v} = \dot{\gamma}(y, -x, 0)$, follows the same steps as for a pure shear flow with the result

$$\mathbf{h} \cong -\frac{\pi^2 \tau q_0^2 k_B T}{\xi_\parallel}(\boldsymbol{\omega}\times\hat{\mathbf{n}}) + \frac{\pi^2}{12}\frac{\tau^2 q_0^2}{\xi_\parallel} k_B T \boldsymbol{\omega}\times(\boldsymbol{\omega}\times\hat{\mathbf{n}}) + O(\dot{\gamma}\tau)^3\,, \tag{4.29}$$

where $\boldsymbol{\omega} = \dot{\gamma}\hat{\mathbf{z}}$. The proper "covariant" generalization is

$$\mathbf{h} \cong \left[\frac{\pi^2 \tau q_0^2 k_B T}{\xi_\parallel}\right]\mathbf{N} + \left[\frac{\pi^2}{12}\frac{\tau^2 q_0^2 k_B T}{\xi_\parallel}\right]\frac{d\mathbf{N}}{dn}\,, \tag{4.30}$$

where $\mathbf{N} = \partial\mathbf{n}/\partial t - \boldsymbol{\omega}\times\mathbf{n}$. Using Eq. (4.30) in Eq. (4.28) gives the renormalization

$$\gamma_1^R \cong \gamma_1 + \frac{\pi^2 q_0^2 \tau}{\xi_\parallel} k_B T \tag{4.31}$$

from which Eq. (4.14c) follows. The covariant correction deriving from the $d\mathbf{N}/dt$ term in Eq. (4.30) leads to an effective inertial term. More precisely, we must generalize Eq. (4.28) to

$$\hat{\mathbf{n}} \times \left[\gamma_1^R \mathbf{N} - I^R \frac{d\mathbf{N}}{dt}\right] = 0 \tag{4.32}$$

with

$$I^R = \frac{\pi^2 \tau^2 q_0^2 k_B T}{\xi_\parallel} \tag{4.33}$$

acting as an effective moment of inertia. However, as long as the precession rate ω_0 is small compared to the shear rate $\dot{\gamma}$, these induced inertia terms can be neglected. Near $T_{N\text{-Sm-}A}$ as well as near T_t, ω_0 vanishes so the assumption $\omega_0/\dot{\gamma} \ll 1$ is valid in the most interesting temperature regimes. We thus will retain Eq. (4.13) with $\mathbf{h}$ the static normal torque, except that we always must obey Eq. (4.14c) for γ_1^R.

D. Stiffness constants under shear flow

The dependence of the α_3 viscosity on shear rate and the appearance of the normal torque were all consequences of the spatially averaged fluctuation torque. If we want to know the effect of shear flow on the stiffness constants then we have to consider the wave-vector dependence of the molecular field. We first recall that, formally, a nematic liquid crystal near $T_{N\text{-Sm-}A}$ can be mapped[33] onto a normal metal close to a phase transition into the superconducting phase. The smectic order parameter ψ turns into the complex Ginzburg-Landau order parameter for superconductivity and the director field into the vector potential. More precisely, if we as-

sume that on average $\hat{\mathbf{n}}=\hat{\mathbf{z}}$ (a orientation) and that $\Psi(\mathbf{r})\propto\exp(iq_0z)$, we can expand

$$\hat{\mathbf{n}}=\hat{\mathbf{z}}+\delta\hat{n}(\mathbf{r}) , \tag{4.34a}$$

$$\psi(\mathbf{r})=\varphi(\mathbf{r})\exp(iq_0z) \tag{4.34b}$$

and use Eq. (4.34) in Eq. (3.1). This gives the free-energy cost F of a fluctuation:

$$F=\int d^3r\left[C_{\parallel}\left|\frac{\partial\varphi}{\partial z}\right|^2+C_{\perp}|(\nabla_{\perp}-iq_0\delta\hat{\mathbf{n}})\varphi|^2+A|\varphi|^2 +\tfrac{1}{2}K_1(\nabla\cdot\delta\hat{\mathbf{n}})^2+\tfrac{1}{2}K_2[\hat{\mathbf{z}}\cdot(\nabla\times\delta\hat{\mathbf{n}})]^2 +\tfrac{1}{2}K_3(\nabla\times\delta\hat{\mathbf{n}})^2\right] , \tag{4.35}$$

where we added the usual Frank free-energy cost of a nonuniform director field. We will choose $\delta\hat{\mathbf{n}}(\mathbf{r})=\delta\hat{\mathbf{n}}(\mathbf{k})e^{i\mathbf{k}\cdot\mathbf{r}}$. Under the mapping

$$\frac{2e\,\mathbf{A}}{\hbar c}\Longrightarrow q_0\delta\hat{\mathbf{n}},\quad \frac{\hbar^2}{2m}\Longrightarrow C$$

(with $C_{\parallel}=C_{\perp}=C$) ΔF is transformed into the Ginzburg-Landau free energy of a superconductor.

The molecular field $\mathbf{h}=-\delta F/\delta\hat{\mathbf{n}}$ is given by

$$h_{\alpha}(\mathbf{k})=-[K_{\alpha}(k_x^2+k_y^2)+K_3k_z^2]\delta\hat{\mathbf{n}}_{\alpha}(\mathbf{k}) +C_{\perp}q_0\int d^3\mathbf{q}[q_{\alpha}\varphi_{\mathbf{q}}\varphi^*_{\mathbf{q}-\mathbf{k}}-q_0|\varphi_{\mathbf{q}}|^2\delta n_{\alpha}(\mathbf{k})+\text{c.c.}] , \tag{4.36}$$

where $\alpha=x,y$ and where $\varphi_{\mathbf{q}}$ is the Fourier transform of $\varphi(\mathbf{r})$. Under the mapping $\hbar\mathbf{j}/2e\Longrightarrow q_0^{-1}\mathbf{h}$ it transforms into the diamagnetic current $\mathbf{j}=-c\,\partial F/\partial\,\mathbf{A}$ given by

$$\mathbf{j}=-\frac{ie\hbar}{m}(\psi^*\nabla\psi-\psi\nabla\psi^*)-\frac{4e^2}{mc}|\psi|^2\mathbf{A} . \tag{4.37}$$

In the absence of shear flow, one can now directly exploit this relationship to find the renormalization of the stiffness constant.[33] The diamagnetic current of a superconductor is of the form $\chi_d\nabla\times(\nabla\times\mathbf{A})$. The diamagnetic susceptibility diverges at the critical temperature by an amount proportional to the superconducting correlation length.[34] In the same way, the molecular field, for $\dot{\gamma}=0$, has the form

$$\mathbf{h}(\mathbf{k})\sim-Kk^2\delta n(\mathbf{k}) \tag{4.38}$$

with K diverging at $T_{N\text{-Sm-}A}$ by an amount proportional to ξ. For $\dot{\gamma}=0$ the mapping gives[33]

$$K_3\propto q_0^2k_BT\xi_{\parallel} . \tag{4.39}$$

We now would like to know the effect of shear flow on Eq. (4.39). The operator $\dot{\gamma}y\partial/\partial x$ has, unfortunately, no direct analog in the theory of superconductivity. However, we can still employ the same method used by Schmid[34] in computing χ_d to find K_3 under shear flow.

Assume, for simplicity, that $\hat{\mathbf{n}}=\hat{\mathbf{z}}+\hat{\mathbf{x}}\delta n_xe^{ikz}$. Then, from Eq. (4.30),

$$h_x(k)=-K_3k^2\delta n_x +C_{\perp}q_0\int d^3q(q_x\langle\varphi_{\mathbf{q}}\varphi^*_{\mathbf{q}-\mathbf{k}}\rangle -q_0\delta n_x\langle|\varphi_{\mathbf{q}}|^2\rangle+\text{c.c.}) . \tag{4.40}$$

We replaced $\varphi_{\mathbf{q}}\varphi^*_{\mathbf{q}-\mathbf{k}}$ by its expectation value $\langle\varphi_{\mathbf{q}}\varphi^*_{\mathbf{q}-\mathbf{k}}\rangle$. If we expand $h_x(k)$ in powers of k then the lowest-order ($k=0$) contribution to Eq. (4.40) was already considered in Eq. (4.9). The next-order term is proportional to k^2 and can be absorbed into a redefinition of K_3:

$$K_3^R=K_3-\tfrac{1}{2}C_{\perp}q_0\frac{\partial^2}{\partial k^2}\frac{\partial}{\partial\delta n_x}\int d^3q\,q_x(\langle\varphi_{\mathbf{q}}\varphi^*_{\mathbf{q}-\mathbf{k}}\rangle+\text{c.c.}) . \tag{4.41}$$

It is now immediately clear from the preceding sections that $K_3^R=K_3$ for $\dot{\gamma}\tau\rightarrow\infty$ since fluctuations are suppressed in the regime of large Deborah numbers.

We are thus required to compute the "vertex" $\langle\varphi_{\mathbf{q}}\varphi^*_{\mathbf{q}-\mathbf{k}}\rangle$. The calculation follows the same steps as discussed in the calculation of $S(\mathbf{q})$ and is discussed in Appendix E. Like $S(\mathbf{q})$, the vertex obeys a differential equation:

$$\left[\Gamma(\mathbf{q})-\dot{\gamma}q_x\frac{\partial}{\partial q_y}\right]\langle\varphi_{\mathbf{q}}\varphi^*_{\mathbf{q}-\mathbf{k}}\rangle =2q_0C_{\perp}\delta n_xq_xS(\mathbf{q}-\mathbf{k}+q_0\hat{\mathbf{z}})/\gamma_3 , \tag{4.42}$$

where

$$\Gamma(\mathbf{q})=[A+C_{\parallel}q_z^2+C_{\perp}(q_x^2+q_y^2)]/\gamma_3 . \tag{4.43}$$

For $\dot{\gamma}=0$, the solution of Eq. (4.42) is obvious:

$$\langle\varphi_{\mathbf{q}}\varphi^*_{\mathbf{q}-\mathbf{k}}\rangle_0=\frac{2q_0C_{\perp}\delta n_xq_x}{(2\pi)^3\gamma_3^2}\frac{1}{\Gamma(\mathbf{q})}\frac{k_BT}{\Gamma(\mathbf{q}-\mathbf{k})} \tag{4.44}$$

so

$$\frac{\partial^2}{\partial k^2}\frac{\partial}{\partial\delta n_x}\langle\varphi_{\mathbf{q}}\varphi^*_{\mathbf{q}-\mathbf{k}}\rangle_0=\frac{2q_0}{(2\pi)^3}\frac{C_{\perp}q_xk_BT}{\gamma_3^2\Gamma(\mathbf{q})}\frac{\partial^2}{\partial q_z^2}\left[\frac{1}{\Gamma(\mathbf{q})}\right] . \tag{4.45}$$

If we use this in Eq. (4.41), we can find the twist elastic constant for $\dot{\gamma}=0$:

$$K_3^R(0)=K_3+\frac{2C_{\perp}^2q_0^2k_BT}{(2\pi)^3\gamma_3^2}\int d^3\mathbf{q}\,q_x^2\left[\frac{\partial}{\partial q_z}\frac{1}{\Gamma(\mathbf{q})}\right]^2 . \tag{4.46}$$

The twist elastic constant is, as expected, enhanced by shear flow. Using Eq. (4.46) gives

$$K_3^R(0)=K_3+\frac{1}{24\pi}q_0^2k_BT\xi_{\parallel} . \tag{4.47}$$

This is the well-known result of de Gennes according to which K_3^R diverges as $\xi_{\parallel}$ at $T_{N\text{-Sm-}A}$.[33]

The first-order correction in $\dot{\gamma}\tau$ to $\langle\varphi_{\mathbf{q}}\varphi^*_{\mathbf{q}-\mathbf{k}}\rangle$ is odd in q_x and does not contribute to the integral in Eq. (4.41).

The second-order term gives, after a tedious calculation (Appendix E),

$$K_3^R(\dot\gamma)\simeq K_3^R(0)-0.016q_0^2k_BT\xi_\parallel(\dot\gamma\tau)^2 \ . \tag{4.48}$$

Comparing Eqs. (4.48) and (4.47), we see that the twist stiffness constant "softens" under shear flow, in particular when $\dot\gamma\tau$ approaches 1. We did not consider other orientations for $\hat{\mathbf{n}}$ or $\mathbf{k}$ but we expect that in the b orientation the softening of K_3^R will start when $\dot\gamma\tau q_0\xi$ is of order 1, just as for α_3^R. The K_2 stiffness constant can be treated similarly.

The correction terms in Eq. (4.40) are not *necessarily* only renormalizations of K_2 and K_3 because the shear flow breaks the rotational symmetry. The remaining symmetry operations require that the free energy is invariant under simultaneous reflection in the $x=0$ (or $y=0$) plane and "time reversal" $\dot\gamma\to-\dot\gamma$. This allows new terms in $\mathbf{h}$ of the form $A(\dot\gamma\tau)k_xk_yn_\alpha(\mathbf{k})$ with $A(x)$ an odd function of x. We will not, however, pursue this question in the present paper.

V. PHASE DIAGRAM

We now turn to the mean-field phase diagram of the Sm-A–N transition under shear flow. We will deduce the critical temperature from the condition that at $T_{N\text{-Sm-}A}$, $S(\mathbf{q})$ must diverge for some $\mathbf{q}^*$. This of course assumes that the transition remains continuous under shear, which appears to be the case experimentally.

The first thing to note is that in the presence of shear, $T_{N\text{-Sm-}A}$ must depend on the orientation of the director with respect to the flow field. Since, as we saw, the director can assume more than one orientation, this leads to some indeterminacy in $T_{N\text{-Sm-}A}$ if in a given sample more than a single orientation of $\hat{\mathbf{n}}$ is realized. The next important issue is the fact that we are at the lower critical dimension of the smectic phase. Thermal fluctuations, which at zero shear reduce $T_{N\text{-Sm-}A}$, are suppressed so $T_{N\text{-Sm-}A}$ is expected to increase under shear flow towards the mean-field transition temperature $T^{\rm MF}$.

To compute this increase, we must include a fourth-order $|\psi|^4$ term in the free energy:

$$F=\int d^3r[\,A|\psi|^2+B|\psi|^4+C_\parallel|(\hat{\mathbf{n}}\cdot\nabla-iq_0)\psi|^2 +C_\perp|(\hat{\mathbf{n}}\times\nabla)\psi|^4]+\cdots \ . \tag{5.1}$$

The fourth-order term will be included through the Hartree approximation, i.e., we replace it by $2B|\psi|^2\langle|\psi^2|\rangle$, with $\langle|\psi|^2\rangle$ the average of $|\psi|^2$. In the absence of fluctuations $A(T)=A'(T-T^{\rm MF})$. The actual transition temperature for $\dot\gamma=0$ in the Hartree approximation is

$$T_{N\text{-Sm-}A}(0)=T^{\rm MF}-\frac{2B}{A'}\langle|\psi^2|\rangle \ . \tag{5.2}$$

In terms of the structure factor $S(\mathbf{q})$,

$$T_{N\text{-Sm-}A}(0)=T^{\rm MF}-\frac{2B}{A'}\int d^3q\,S(\mathbf{q}) \ . \tag{5.3}$$

We now turn to the transition temperature in the presence of flow. From Eq. (3.19), we can draw an important consequence. The integral is finite whenever β is nonzero. This means that $S(\mathbf{q})$ can *only* diverge for $q_x=0$. The condition for a divergence in Eq. (3.19) is then

$$\Gamma_0(0,q_y^*,q_z^*)=0 \tag{5.4}$$

with, in the definition of $\Gamma_0(\mathbf{q})$, A everywhere replaced by $A+2B\langle|\psi|^2\rangle$. As we lower T, the highest temperature where Eq. (5.4) is satisfied is, for $\hat{\mathbf{n}}=\hat{\mathbf{z}}+\delta\hat{\mathbf{n}}$,

$$A+2B\langle|\psi^2|\rangle+C_\perp q_0^2\delta n_x^2=0 \tag{5.5}$$

while the divergence is at

$$\mathbf{q}^*\simeq q_0(0,\delta n_y,1) \ . \tag{5.6}$$

The critical temperature is then

$$T_{N\text{-Sm-}A}(\dot\gamma)=T^{\rm MF}-\frac{2B}{A'}\int d^3q\,S(q)-\left[\frac{C_\perp q_0^2\delta n_x^2}{A'}\right] . \tag{5.7}$$

From our limiting expression for $S(\mathbf{q})$ for small Deborah number we find, using Eqs. (5.2) and (3.26),

$$T_{N\text{-Sm-}A}(\dot\gamma)\cong T_{N\text{-Sm-}A}(0)+\frac{1}{96\pi}\frac{B}{A'}\frac{k_BT(\dot\gamma\tau)^2}{C_\perp\xi_\parallel} -\frac{C_\perp q_0^2}{A'}\delta n_x^2 \ . \tag{5.8}$$

For $\delta n_x=0$, shear flow increases the transition temperature by an amount proportional to $(\dot\gamma\tau)^2$. It should be recalled here that Onuki and Kawasaki found, for shear flow in a binary-fluid mixture, a *reduction* in T_c due to fluctuation corrections to mean-field theory. The reduction was proportional to $\epsilon^{0.53}(\dot\gamma)$ with $\epsilon=4-d$. Similar corrections are expected for our case as well.

Even if $\hat{\mathbf{n}}$ is oriented perpendicular to the flow direction, there is still a contribution from the last term in Eq. (5.8) due to thermal fluctuations of the director. In the spirit of mean-field theory, we can estimate this effect by replacing δn_x^2 by its thermal average $\langle\delta n_x^2\rangle$, and using Eq. (3.26):

$$T_{N\text{-Sm-}A}(\dot\gamma)\cong T_{N\text{-Sm-}A}(0)-\frac{2B}{A'}(\langle|\psi^2|\rangle-\langle|\psi|^2\rangle_{\dot\gamma=0}) -\frac{Cq_0^2}{A'}\langle\delta n_x^2\rangle \ . \tag{5.9}$$

We will not compute the shear-rate dependence of $\langle\delta n_x^2\rangle$, but only speculate on the qualitative behavior. For $\dot\gamma\tau\ll1$, $\langle\delta n_x^2\rangle$ should *decrease* with shear rate because of the shear-induced gap in the fluctuation spectrum of the director. For $\dot\gamma\tau\gtrsim1$, the $\hat{\mathbf{z}}$ orientation destabilizes [Eq. (4.14a)] while the stiffness constants are reduced according to Eq. (4.48). We thus expect that $\langle\delta n_x^2\rangle$ starts to *increase* around $\dot\gamma\tau=1$ since the fluctuations in δn_x are becoming large.

Returning to Eq. (5.9), since both $\langle|\psi|^2\rangle$ and $\langle\delta n_x^2\rangle$ initially decrease with $\dot\gamma$ for $\dot\gamma\tau\ll1$, we expect $T_{N\text{-Sm-}A}(\dot\gamma)$ to indeed be an increasing function of shear

rate. For $\dot{\gamma}\tau \gtrsim 1$, $\langle |\psi|^2 \rangle$ will have become very small while $\langle \delta n_x^2 \rangle$ is growing. This leads us to expect that $T_{N\text{-Sm-}A}$ will decrease with $\dot{\gamma}$ for $\dot{\gamma}\tau > 1$, so we predict a *reentrant* phase diagram. For temperatures T slightly above $T_{N\text{-Sm-}A}(0)$ we encounter, with increasing shear rate, the smectic phase at $T = T_{N\text{-Sm-}A}(\dot{\gamma})$. For larger shear rates ($\dot{\gamma}\tau > 1$) we should return to the nematic phase.

VI. CONCLUSION

In this paper we have studied the effect of shear flow on the nematic phase near the nematic to smectic-A phase transition. We found that when the external flow rate $\dot{\gamma}$ exceeded the order-parameter decay rate τ^{-1}, the imposed flow field altered the spatial nature of the pretransitional smectic-A fluctuation clusters. Therefore, by measuring the dimensions of the distorted cluster through the x-ray structure factor, one can obtain the dynamical relaxation time $\tau(\dot{\gamma})$ of the fluctuations with use of an inherently static probe. Because of the internal length scale of the smectic density wave, namely, the layer spacing d, we found that the condition for the onset of the distortion of the microscopic fluctuations depends on the relative orientation of the director with respect to the shear plane. We first discuss the case for the a ($\hat{\mathbf{n}} = \hat{\mathbf{z}}$) and c ($\hat{\mathbf{n}} = \hat{\mathbf{y}}$) orientations with the director $\hat{\mathbf{n}}$ normal to the $\hat{\mathbf{x}}$ flow direction. The gradient velocity direction is taken along the $\hat{\mathbf{y}}$ direction.

For large Deborah numbers $\dot{\gamma}\tau > 1$, we found a regime in reciprocal-$\mathbf{q}$ space where $S(\mathbf{q})$ (the Fourier transform of the density-density correlation function which describes a cluster) is highly distorted. Outside of this regime $S(\mathbf{q})$ is not affected. The bounds of this regime form an anisotropic surface in $\mathbf{q}$ space ($\mathbf{q} = \mathbf{q}_s$) which is determined by both the shear rate $\dot{\gamma}$ and the reduced temperature $t = (T - T_{N\text{-Sm-}A})/T_{N\text{-Sm-}A}$. Physically, this regime consists of those order-parameter fluctuations whose wave vector $\mathbf{q}$ lies inside this surface, and satisfies the condition $\dot{\gamma}\tau(\mathbf{q}) > 1$; these fluctuations are sheared before they dissipate thermally. (Alternatively, one may say that shear flow will distort those clusters for which the equilibrium correlation length ξ exceeds this new length scale $|\mathbf{q}_s|^{-1}$, because they will live long enough to feel the effects of shear.) We found that for $\dot{\gamma}\tau > 1$, $|\mathbf{q}_s|$ grows rapidly, and the onset of distortion in $S(\mathbf{q})$ sets in over a narrow temperature range in the vicinity of $T_{N\text{-Sm-}A}$. This sudden onset of distortion is due to the *nonconserved* nature of the smectic-A order parameter for this transition. Onuki and Kawasaki found that for the binary-fluid phase transition, which is described by a *conserved* order parameter (the concentration), the growth in $\mathbf{q}_s$ begins at $\dot{\gamma}\tau = 0$, and therefore the distortion of $S(\mathbf{q})$ as a function of temperature occurs gradually over a larger temperature range.[9]

For $\dot{\gamma}\tau \gg 1$ in the distorted regime, the fluctuations become extremely anisotropic possessing an effectively very large correlation length $\approx \dot{\gamma}\tau\xi$ along the flow direction. In this novel limit, for length scales less than $\dot{\gamma}\tau\xi$, the density-density correlations are extended and decrease algebraically (that is, they exhibit quasi-long-range order) along the flow direction, while they are cut off in the plane normal to the flow direction. The real-space structure would correspond to one-dimensional strings of distorted clusters.

For the b orientation when the director ($\hat{\mathbf{n}} = \hat{\mathbf{x}}$) lies along the flow direction, the internal length scale $d \sim q_0^{-1}$ (which has no analog in the binary-fluid problem) becomes important. In this case, we found that the distortion in $S(\mathbf{q})$ starts when $\dot{\gamma}\tau q_0 \xi$ is of order 1 (rather than our previous condition of $\dot{\gamma}\tau \simeq 1$). Thus we predict that the onset of distortion of the clusters occurs significantly earlier as one approaches $T_{N\text{-Sm-}A}$ from the nematic phase, because $q_0\xi$ is much larger than 1 over most of the temperature range in the nematic phase.[13,14] In general, we found that the distortion always results in a *suppression* of fluctuations by shear flow and that the magnitude of the order-parameter fluctuations $\sim \int d^3q\, S(\mathbf{q}, \dot{\gamma} \neq 0)$ tends to zero as $\dot{\gamma}\tau \gg 1$. This was also found by Onuki and Kawasaki in their studies of binary fluids under shear flow. Thus we expect that fluctuation domains with the b orientation are suppressed earlier than those with the a and c orientations. A similar orientational dependence in the suppression of fluctuations was also found by Cates and Milner in their analysis of the isotropic to the lamellar L_α phase-transition in surfactant systems.[15]

Aside from the effect of shear on the microscopic pretransitional fluctuations associated with the transition, a number of *macroscopic* static and dynamic properties of the nematic phase are also affected by shear. These include both the elastic and transport coefficients of the nematic phase in the vicinity of the nematic to smectic-A phase-transition temperature. At equilibrium, the presence of the fluctuation clusters results in a renormalized stiffening of the nematic bend and twist elastic constants K_3 and K_2. This is because a bend or twist mode of the nematic director results in a change of the layer spacing of the cluster which is energetically costly. Additionally, the viscosity coefficient α_3 (proportional to η_b) measured in the b orientation with the director along the flow is increased in the presence of the domains since shear flow will tend to tilt the layers, which changes the layer spacing and is unfavorable. We found that shear flow leads to a reduction of the renormalized elastic constants K_2 and K_3 towards their bare high-temperature nematic values. Similarly, α_3 is also reduced by shear flow for $\dot{\gamma}\tau q_0 \xi \sim 1$. This is the analog of *shear thinning* that is commonly encountered in polymeric fluids and signals the onset of non-Newtonian behavior. What is interesting is that we are able to directly correlate the underlying microscopic mechanism (that is, the suppression of the fluctuations due to shear), responsible for the thinning of the macroscopic transport coefficient.

The shear thinning of α_3 has an important consequence regarding the director orientation under shear flow. At low Deborah numbers near $T_{N\text{-Sm-}A}$, the fluctuation renormalized α_3 is positive, and the director chooses the a orientation (normal to the flow). We found that any deviation away from this direction results in a fluctuation

torque which tends to reorient the director back along the a orientation. However, when shear thinning sets in, around $\dot{\gamma}\tau q_0\xi \approx 1$, α_3 is reduced to its bare negative value, and the b orientation becomes a stable solution. The stability of the a orientation is unaffected so we predict a *regime of coexistence for the a and b orientations which sets in for* $\dot{\gamma}\tau q_0\xi \simeq 1$ and extends to $\dot{\gamma}\tau \simeq 1$.

The temperature–shear-rate phase diagram also shows interesting behavior. At equilibrium, the nematic to smectic-A transition is at its lower critical dimension.[11] Thus thermal fluctuations should be very important which will tend to reduce the transition temperature $T_{N\text{-Sm-}A}$ substantially below the mean-field transition temperature for the phase transition. First, because shear flow suppresses fluctuations which are primarily responsible for a reduced $T_{N\text{-Sm-}A}$ at zero shear, we find that for increasing shear rates, $T_{N\text{-Sm-}A}$ *increases* towards its mean-field transition temperature. Cates and Milner[15] also found a rise in the isotropic-to-lamellar L_α transition temperature due to the suppression of fluctuations under shear flow. This is in contrast to the binary-fluid problem[9] (where fluctuations are not as important for $\dot{\gamma}=0$), where shear flow always favors the mixed phase and so reduces the transition temperature. However, at very high shear rates, our analysis suggests that the nematic phase is favored to the smectic phase, and so we expect an eventual reduction of $T_{N\text{-Sm-}A}$ for high shear rates. Thus, for temperatures just above $T_{N\text{-Sm-}A}(\dot{\gamma}=0)$, we expect a reentrant behavior from nematic to smectic A and again to the nematic phase as $\dot{\gamma}$ increases.

The analogy between nematic liquid crystals and non-Newtonian polymeric fluids is not restricted to shear thinning. The unusual flow behavior of polymeric liquids is due to normal-stress effects. In Appendix F we show that normal-stress effects also occur near $T_{N\text{-Sm-}A}$. We thus predict that close to $T_{N\text{-Sm-}A}$, a nematic liquid crystal will also exhibit unusual flow behavior (such as the Weissenberg effect[2]).

On a more fundamental level, we showed that, near $T_{N\text{-Sm-}A}$, the nematic director fluctuations acquire a "gap" in their spectrum. The appearance of the gap could be anticipated from general arguments based on symmetry. In the absence of shear flow, the free energy of a nematic liquid crystal must be invariant under uniform global rotations of the director. This requirement leads to the familiar splay, bend, and twist terms. This symmetry is broken in the presence of shear flow. The corresponding Goldstone modes must acquire a gap in their spectrum. In our case this requires a restoring force on the director even for $\mathbf{k}=\mathbf{0}$, i.e., terms in F proportional to δn_α^2. The fact that the rotational symmetry is broken means that the symmetry arguments used to construct the nematic free energy become invalid for finite Deborah numbers. This suggests that the theory of textural defects, thermal fluctuations, and other properties of the nematic phase all should be reconsidered as well under shear flow.

ACKNOWLEDGMENTS

We should like to thank Michael Cates, Paul Chaikin, Geoff Grinstein, Tom Lubensky, Scott Milner, and John Toner for useful discussions. This research was supported in part by the National Science Foundation under Grant No. PHY89-04035, supplemented by funds from the National Aeronautics and Space Administration, at the University of California at Santa Barbara.

APPENDIX A: THE STRUCTURE FACTOR FOR LARGE DEBORAH NUMBERS

In this appendix we obtain the expression for $S(\mathbf{q})$ for large Deborah numbers $\dot{\gamma}\tau \gg 1$. First we rewrite Eq. (3.19):

$$\frac{S(\mathbf{q})}{k_BT/\gamma_3} = \frac{1}{2\pi^3} e^{\beta A^3} \int_0^\infty dt \exp[-\beta(t+A)^3 - Bt] \quad \text{(A1)}$$

with

$$A \equiv \frac{\alpha}{3\beta} ,$$

$$B \equiv \Gamma_0(\mathbf{q}) - \frac{\alpha^2}{3\beta} . \quad \text{(A2)}$$

Next, we change variables twice. First, we set $t+A=y$. Equation (A1) becomes $e^{\beta A^3}\int_A^\infty dy \exp[-\beta y^3 - B(y-A)]$. Second, we set $Z \equiv y^3$, so that Eq. (A1) becomes

$$\frac{S(\mathbf{q})}{k_BT/(2\pi)^3\gamma_3} = \frac{e^{\beta A^3}}{3}\int_{A^3}^\infty dZ\, Z^{-2/3}\exp[-\beta Z - B(Z^{1/3}-A)]$$

$$= \frac{e^{\beta A^3}}{3}\int_{A^3}^\infty dZ\, Z^{-2/3} e^{-\beta Z}\left[1 - B(Z^{1/3}-A) + \frac{B^2(Z^{1/3}-A)^2}{2} + \cdots\right] . \quad \text{(A3)}$$

We point out that the main contribution to the above integral comes for $1/\beta > Z > A^3$. In this range, $B(Z^{1/3}-A)<1$ for $\dot{\gamma}\tau \gg 1$ and the expansion in Eq. (A3) is valid. Collecting terms, we find that

$$\frac{S(\mathbf{q})}{k_BT/(2\pi)^3\gamma_3} = \frac{e^{\beta A^3}}{3}\int_{A^3}^\infty dZ\, Z^{-2/3} e^{-\beta Z} \times \left[C + DZ^{1/3} + \frac{B^2Z^{2/3}}{2}\right] . \quad \text{(A4)}$$

Here,

$$C \equiv 1 + AB + (AB)^2/2 ,$$

and

$$D \equiv -B + AB^2 .$$

Next, we use the identity (see Ref. 35)

$$\int_\mu^\infty x^{\nu-1} e^{-\mu x} dx = \mu^{-\nu}\Gamma(\nu,\mu\nu) \quad (u>0, \mathrm{Re}\mu>0)$$

with

$$\Gamma(\alpha,x)\equiv\Gamma(\alpha)-\sum_{n=0}^{\infty}\frac{(-1)^n x^{\alpha+n}}{n!(\alpha+n)}$$

and $\Gamma(\alpha)$ is the gamma function. The three terms of Eq. (A4) are then easily evaluated, which leads to Eq. (3.29).

APPENDIX B: THE FLUCTUATION TORQUE FOR THE *a* ORIENTATION

To derive Eq. (3.26), it is convenient to first give the result of a formal perturbation expansion of Eq. (3.15):

$$S(\mathbf{q})=S_0(\mathbf{q})+S_1(\mathbf{q})+S_2(\mathbf{q}) , \tag{B1}$$

where

$$S_0(\mathbf{q})=k_BT/(2\pi)^3\gamma_3\Gamma_0(\mathbf{q}) , \tag{B2a}$$

$$S_1(\mathbf{q})=\left[\frac{\dot\gamma}{\Gamma_0(\mathbf{q})}q_x\frac{\partial}{\partial q_y}\right]S_0(\mathbf{q}) , \tag{B2b}$$

$$S_2(\mathbf{q})=\left[\frac{\dot\gamma}{\Gamma_0(\mathbf{q})}q_x\frac{\partial}{\partial q_y}\right]^2 S_0(\mathbf{q}) , \tag{B2c}$$

$$\vdots$$

We must compute

$$\langle|\psi|^2\rangle=\int d^3q\, S(\mathbf{q}) \tag{B3}$$

for $\hat{\mathbf{n}}=\hat{\mathbf{z}}$. The first term gives $\langle|\psi|^2\rangle_{\dot\gamma=0}$, the value of $\langle|\psi|^2\rangle$ for $\dot\gamma=0$. Since for $\hat{\mathbf{n}}=\hat{\mathbf{z}}$

$$\Gamma_0(\mathbf{q})=[A+C_\parallel(q_z-q_0)^2+C_\perp(q_x^2+q_y^2)]/\gamma_3 \tag{B4}$$

is even, there is no contribution from S_1. The contribution of S_2 is

$$\begin{aligned}\langle|\psi|^2\rangle-\langle|\psi^2|\rangle_{\dot\gamma=0}&=\int d^3q\left[\frac{\dot\gamma}{\Gamma_0(\mathbf{q})}q_x\frac{\partial}{\partial q_y}\right]^2\frac{k_BT}{\Gamma_0(\mathbf{q})\gamma_3}\\&=-2\dot\gamma^2\frac{k_BT}{(2\pi)^3\gamma_3}\\&\quad\times\int d^3q\frac{q_x^2}{\Gamma_0(\mathbf{q})}\left[\frac{\partial}{\partial q_y}\frac{1}{\Gamma_0(\mathbf{q})}\right]^2 ,\end{aligned} \tag{B5}$$

where the second expression is obtained after partial integration by q_y. After performing the derivative one finds

$$\begin{aligned}\langle|\psi|^2\rangle-\langle|\psi|^2\rangle_{\dot\gamma=0}&=-2(2\gamma_3\dot\gamma C_\perp)^2k_BT\int d^3q\frac{q_x^2q_y^2}{\Gamma_0(\mathbf{q})^5\gamma_3^5}\\&=-\frac{2(2\gamma_3\dot\gamma C_\perp)^2k_BT}{(2\pi)^3A^5\xi_\parallel\xi_\perp^6}\\&\quad\times\int d^3r\frac{x^2y^2}{(1+|\mathbf{r}|^2)^5} ,\end{aligned} \tag{B6}$$

where we redefined $x=\xi_\perp q_x$, $y=\xi_\perp q_y$, and $z=\xi_\parallel q_z$ in the second step. The integral is straightforward and gives $\pi^2/192$. After using $\gamma_3/A=\tau$, we find Eq. (3.26).

To derive Eq. (4.12), we use Eqs. (B2) in Eq. (4.11), but now with $\hat{\mathbf{n}}=\hat{\mathbf{z}}+\delta\hat{\mathbf{n}}$:

$$\mathbf{h}=2C_\perp q_0\int d^3q(\mathbf{q}-q_0\delta\hat{\mathbf{n}})S(\mathbf{q}+q_0\hat{\mathbf{z}}) . \tag{B7}$$

Equation (B7) is derived from (4.11) by two transformations: first redefine $\mathbf{q}\to\mathbf{q}+q_0\hat{\mathbf{n}}$ where $\hat{\mathbf{n}}=\hat{\mathbf{z}}+\delta\hat{\mathbf{n}}$, then redefine $\mathbf{q}\to\mathbf{q}-q_0\delta\hat{\mathbf{n}}$ to arrive at (B7). (All terms proportional to $\hat{\mathbf{n}}$ are dropped since the torque is $\hat{\mathbf{n}}\times\mathbf{h}$.) We will use the perturbation expansion of $S(\mathbf{q})$ given by (B1) to evaluate (B7) term by term. First, it is straightforward to show that S_0 does not contribute to $\mathbf{h}$. The first-order term $\mathbf{h}^{(1)}$ is

$$\mathbf{h}^{(1)}=-\frac{4C_\perp q_0k_BT}{(2\pi)^3}\int d^3q(\mathbf{q}-q_0\delta\hat{\mathbf{n}})\frac{\alpha(\mathbf{q}+q_0\hat{\mathbf{z}})}{\Gamma_0^3(\mathbf{q}+q_0\hat{\mathbf{z}})\gamma_3^2} , \tag{B8}$$

where

$$\alpha(\mathbf{q}+q_0\hat{\mathbf{z}})=\dot\gamma C_\perp q_x\left[q_y-(q_z+q_0)\delta n_y+\frac{C_\parallel}{C_\perp}q_z\delta n_y\right]\Big/\gamma_3 \tag{B9}$$

and where, to lowest order in $\delta\hat{\mathbf{n}}$,

$$\begin{aligned}\Gamma_0(\mathbf{q}+q_0\hat{\mathbf{z}})=[&A+C_\parallel(q_z+\delta\hat{\mathbf{n}}\cdot\mathbf{q}_\perp)^2\\&+C_\perp(\mathbf{q}_\perp-(q_0+q_z)\delta\hat{\mathbf{n}})]^2/\gamma_3 .\end{aligned} \tag{B10}$$

Substituting (B9) and (B10) into (B8), we find

$$\mathbf{h}^{(1)}=-\frac{4C_\perp^2q_0k_BT}{(2\pi)^3}\gamma_3\dot\gamma\int d^3\mathbf{q}\frac{(\mathbf{q}-q_0\delta\hat{\mathbf{n}})q_x\left[q_y-q_0\delta n_y+q_z\delta n_y\left[\frac{C_\parallel}{C_\perp}-1\right]\right]}{\Gamma_l^3(1+\Delta/\Gamma_l)^3} , \tag{B11}$$

where $\Gamma_l\equiv A+C_\parallel q_z^2+C_\perp(\mathbf{q}_\perp-q_0\delta\mathbf{n})^2$ and $\Delta\equiv2\delta\hat{\mathbf{n}}\cdot\mathbf{q}_\perp q_z(C_\parallel-C_\perp)$. We define $z=\xi_\parallel q_z$, $x=\xi_\perp(q_x-q_0\delta n_x)$, and $y=\xi_\perp(q_y-q_0\delta n_y)$. It is easy to see that to lowest order in $\delta\mathbf{n}$, only the y component of $\mathbf{h}^{(1)}$ survives (all other terms vanish by symmetry):

$$h^{(1)}|_y=\frac{-4q_0^2k_BT\gamma_3\dot\gamma\delta n_x}{(2\pi)^3A\xi_\parallel}\int d^3r\frac{y^2}{(1+|\mathbf{r}|^2)^3} . \tag{B12}$$

The integral is equal to $\pi^2/4$ so

$$h^{(1)}|_y=\frac{-\pi^2 q_0^2 k_B T(\dot\gamma\tau)\delta n_x}{(2\pi)^3\xi_\parallel} \ . \tag{B13}$$

The second-order term, using Eqs. (B2c) and (B7), is

$$\mathbf{h}^{(2)}=2C_\perp q_0\int d^3\mathbf{q}(\mathbf{q}-q_0\delta\hat{\mathbf{n}})\left[\frac{\dot\gamma q_x}{\Gamma_0}\frac{\partial}{\partial q_y}\right]^2 S_0 \ , \tag{B14}$$

where Γ_0 and S_0 are evaluated at $\mathbf{q}+q_0\hat{\mathbf{z}}$. The $\hat{\mathbf{x}}$ component is, after partial integration,

$$h^{(2)}|_x=-\frac{2C_\perp q_0 k_B T}{(2\pi)^3}(\gamma_3\dot\gamma)^2\int d^3\mathbf{q}\, q_x^2(q_x-q_0\delta n_x)\frac{1}{\Gamma_0\gamma_3}\left[\frac{\partial}{\partial q_y}\frac{1}{\Gamma_0\gamma_3}\right]^2 . \tag{B15}$$

Since

$$\gamma_3\frac{\partial\Gamma_0}{\partial q_y}=2C_\perp\left[q_y-q_0\delta n_y+q_z\delta n_y\left[\frac{C_\parallel}{C_\perp}-1\right]\right] ,$$

to lowest order in $\delta\hat{\mathbf{n}}$,

$$h^{(2)}|_x=-\frac{C_\perp^3}{\pi^3}\frac{q_0 k_B T}{\gamma_3^5}(\gamma_3\dot\gamma)^2\int d^3q\, q_x^2\frac{(q_x-q_0\delta n_x)\left[q_y-q_0\delta n_y+q_z\delta n_y\left[\frac{C_\parallel}{C_\perp}-1\right]\right]^2}{\Gamma_l^5(1+\Delta/\Gamma_l)^5} \ . \tag{B16}$$

The remaining integral is evaluated in the same fashion as in Eq. (B12) with the result

$$h^{(2)}|_x=-\frac{1}{96\pi}q_0^2\frac{k_B T}{\xi_\parallel}(\dot\gamma\tau)^2\delta n_x \ . \tag{B17}$$

Following the same procedure, we find that $h^{(2)}|_y$ and $h^{(2)}|_z$ do not contribute at the lowest order. Finally, the third-order term is

$$\mathbf{h}^{(3)}=2C_\perp q_0\int d^3\mathbf{q}(\mathbf{q}-q_0\delta\hat{\mathbf{n}})\left[\frac{\dot\gamma q_x}{\Gamma_0}\frac{\partial}{\partial q_y}\right]^3 S_0 \ . \tag{B18}$$

The y component gives

$$h^{(3)}|_y=\frac{2C_\perp q_0}{(2\pi)^3}\frac{(\dot\gamma\gamma_3)^3}{\gamma_3^4}k_B T\int d^3\mathbf{q}(q_y-q_0\delta n_y)q_x^3\left[\frac{12C_\perp}{\gamma_3(\Gamma_l+\Delta)^6}\left[\frac{\partial\Gamma_0}{\partial q_y}\right]-\frac{6}{(\Gamma_l+\Delta)^7}\left[\frac{\partial\Gamma_0}{\partial q_y}\right]^3\right] , \tag{B19}$$

where $\partial\Gamma_0/\partial q_y$ is evaluated at $\mathbf{q}+q_0\hat{\mathbf{z}}$. Again, we make a similar transformation used in evaluating (B12) to obtain

$$h^{(3)}|_y=\frac{9}{640\pi}\pi^2 q_0^2(\dot\gamma\tau)^3\frac{k_B T}{\xi_\parallel}\delta n_x \ . \tag{B20}$$

To lowest order $h^{(3)}|_x$ and $h^{(3)}|_z$ are nonzero.

For large Deborah numbers, the integration in $\mathbf{q}$ space in Eq. (B7) must be broken up into the regions I–III defined in Sec. III. We start with region I where $|q_x|\lesssim 1/\xi_\perp\dot\gamma\tau$:

$$\mathbf{h}^{\mathrm{I}}\simeq 2C_\perp q_0\int_{-1/\xi^+}^{+1/\xi^+}dq_x\int dq_y\int dq_z(\mathbf{q}-q_0\delta\hat{\mathbf{n}})S(\mathbf{q}+q_0\hat{\mathbf{z}}) \ , \tag{B21}$$

where $\xi^+=\xi_\perp\dot\gamma\tau$. Even though S_0 is symmetric in $\mathbf{q}-q_0\delta\hat{\mathbf{n}}$, we do get a contribution from S_0 since the integration is not over all of $\mathbf{q}$ space. Define new coordinates

$$\begin{aligned}\tilde q_x&=q_x-q_0\delta n_x \ ,\\ \tilde q_y&=q_y-q_0\delta n_y \ ,\\ \tilde q_z&=q_z \ .\end{aligned} \tag{B22}$$

To lowest order in $\delta\hat{\mathbf{n}}$, $\mathbf{h}^{\mathrm{I}}=\mathbf{h}^0$, with

$$\mathbf{h}^0\simeq 2C_\perp q_0\int_{-1/\xi^+-q_0\delta n_x}^{1/\xi^+-q_0\delta n_x}d\tilde q_x\int d\tilde q_y\int d\tilde q_z(\tilde q_x,\tilde q_y)\frac{k_B T}{A+C_\parallel\tilde q_z^2+C_\perp\tilde q_\perp^2} \ . \tag{B23}$$

Only the integral over $\tilde{q}_x$ is asymmetric so $h_y^0=0$. The integral over $\tilde{q}_x$ gives

$$h_x^0 \simeq \int d\tilde{q}_y \int d\tilde{q}_z C_\perp q_0 k_B T \ln \left[\frac{A + C_\parallel \tilde{q}_z^2 + C_\perp \left[\tilde{q}_y^2 + \left[\frac{1}{\xi^+} - q_0 \delta n_x \right]^2 \right]}{A + C_\parallel \tilde{q}_z^2 + C_\perp \left[q_y^2 + \left[\frac{1}{\xi^+} + q_0 \delta n_x \right]^2 \right]} \right] . \tag{B24}$$

In the limit $\delta n_x \to 0$

$$h_x^0 \approx - \int d\tilde{q}_y \int d\tilde{q}_z \frac{4 C_\perp q_0^2 k_B T \delta n_x / \xi^+}{A + C_\parallel \tilde{q}_z^2 + C_\perp \left[\tilde{q}_y^2 + \frac{1}{\xi^{+2}} \right]} . \tag{B25}$$

The remaining integral has a logarithmic divergence. Let $q_c \approx q_0$ be the large q cutoff. Then

$$h_x^0 \simeq -8\pi \ln(q_c \xi) \frac{q_0^2 k_B T \delta n_x}{\dot{\gamma} \tau \xi_\parallel} . \tag{B26}$$

The first-order correction term S_1 contributes an amount $\mathbf{h}^1$. Only the y component is nonzero. It is given by

$$h_y^1 = \frac{2 C_\perp q_0}{(2\pi)^3 \gamma_3^3} \int_{-1/\xi^+}^{1/\xi^+} dq_x \int dq_y \int dq_z (\mathbf{q} - q_0 \delta \hat{\mathbf{n}})_y \times \frac{-2\alpha(\mathbf{q}) k_B T}{\Gamma_0^3 (\mathbf{q} + q_0 \hat{\mathbf{z}})} . \tag{B27}$$

For $\hat{\mathbf{n}} = \hat{\mathbf{z}}$

$$h_y^1 = -4 C_\perp^2 \frac{k_B T \dot{\gamma}}{(2\pi)^3 \gamma_3^2} q_0 \int_{-1/\xi^+}^{1/\xi^+} dq_x \int dq_y \int dq_z \frac{q_y^2 q_x}{\Gamma_0^3} . \tag{B28}$$

APPENDIX C: NEMATIC HYDRODYNAMICS UNDER SHEAR FLOW

In this appendix, we will briefly discuss some classical results on the dynamics of the nematic director away from the critical temperature. In general, the dynamics is a complex problem because the flow field $\mathbf{v}(\mathbf{r})$ is coupled to the director field $\hat{\mathbf{n}}(\mathbf{r})$. In addition, the viscosity of the nematic liquid crystal is anisotropic. In the simplest case, we can pin $\hat{\mathbf{n}}$ by the boundary conditions and/or magnetic fields and impose an external flow. Miesowicz[25] first measured the previously defined viscosities η_b (along $\hat{\mathbf{n}}$) and η_a and η_c (perpendicular to $\hat{\mathbf{n}}$) under the laminar shear flow defined in Sec. II (Fig. 4). Typical results for p'-methoxybenzylidene-p-n-butylanaline (MBBA) are

$$\begin{aligned} \eta_a &= 41 \times 10^{-2} \text{ P} , \\ \eta_b &= 24 \times 10^{-2} \text{ P} , \\ \eta_c &= 103 \times 10^{-2} \text{ P} , \end{aligned} \tag{C1}$$

so naively one expects to see the b orientation (Fig. 4).

If we now relax the constraints of $\hat{\mathbf{n}}$ then we can study its evolution for a given shear flow. The shear flow exerts a torque on the director and either the director will evolve until it finds an orientation where the torque vanishes, or it performs some periodic motion. It is convenient to first introduce the ELP parameters $\alpha_1 - \alpha_5$.[21-23] In terms of the α's

$$\begin{aligned} \eta_a &= \tfrac{1}{2}\alpha_4 , \\ \eta_b &= \tfrac{1}{2}(\alpha_3 + \alpha_4 + \alpha_6) , \\ \eta_c &= \tfrac{1}{2}(\alpha_4 + \alpha_5 - \alpha_2) . \end{aligned} \tag{C2}$$

If we force the director to lie in the flow plane by applying a magnetic field H, then the torque $\bar{\Gamma}$ was shown by Leslie[22] to be

$$\Gamma_z = \dot{\gamma}(\alpha_3 \cos^2\theta - \alpha_2 \sin^2\theta) \tag{C3}$$

with θ the angle between $\hat{\mathbf{n}}$ and $\hat{\mathbf{v}}$. If we look for static solutions with $\Gamma_z = 0$ then we must demand

$$\tan\theta = (\alpha_3/\alpha_2)^{1/2} . \tag{C4}$$

Measurements of α_2 and α_3 show that $\alpha_2 < 0$. The sign of α_3 depends on temperature. Gähwiller[36] found that α_3 is negative close to the nematic-to-isotropic transition and positive close to $T_{N\text{-Sm-}A}$. This was confirmed by Pieranski and Guyon.[31] Typically, $\theta \approx 10°$ near the temperature T_t where α_3 changes sign. McMillan showed that this sign change of α_3 is related to the appearance of fluctuation clusters near $T_{N\text{-Sm-}A}$. In the regime $T_{N\text{-Sm-}A} < T < T_t$ there is, according to Eq. (C4), no static solution with $\hat{\mathbf{n}}$ constrained to the flow plane.

To find the orientation of $\hat{\mathbf{n}}$ for $\alpha_3 > 0$, we use the equation of motion for $\hat{\mathbf{n}}$ [Eq. (4.7)]:

$$\hat{\mathbf{n}} \times \left[\gamma_1 \frac{\partial}{\partial t} \hat{\mathbf{n}} + \dot{\gamma}(\alpha_2 n_y, \alpha_3 n_x, 0) \right] = \mathbf{0} , \tag{C5}$$

where we set $\mathbf{h}(0) = \mathbf{0}$, i.e., we assume $H = 0$ and we neglect smectic fluctuations. For $\hat{\mathbf{n}} = (\cos\theta, \sin\theta, 0)$, Eq. (C5) gives

$$\gamma_1 \dot{\theta} + \dot{\gamma}(\alpha_3 \cos^2\theta - \alpha_2 \sin^2\theta) = 0 . \tag{C6}$$

If we look for static solutions, we recover Eq. (C4). As mentioned, if $\alpha_2 < 0$ then this is only possible if $\alpha_3 < 0$ as well. For $\alpha_3 > 0$, the director performs a tumbling motion, in the x-y plane. Next, try $\hat{\mathbf{n}}$ close to $\hat{\mathbf{z}}$:

$$\hat{\mathbf{n}} = (n_x, n_y, 1) \tag{C7}$$

with $n_x \ll 1$ and $n_y \ll 1$. Equation (C5) leads to two coupled equations for n_x and n_y:

$$\gamma_1 \dot{n}_x + \dot{\gamma} \alpha_2 n_y = 0 , \tag{C8a}$$

$$\gamma_1 \dot{n}_y + \dot{\gamma}\alpha_3 n_x = 0 \ . \tag{C8b}$$

If $(\alpha_2\alpha_3)<0$, then Eq. (C8) has solutions with $\hat{\mathbf{n}}$ precessing around the $\hat{\mathbf{z}}$ axis:

$$n_x = n_x^0 \cos\left[\frac{\dot{\gamma}}{\gamma_1}(-\alpha_2\alpha_3 t)^{1/2}\right] , \tag{C9a}$$

$$n_y = n_y^0 \sin\left[\frac{\dot{\gamma}}{\gamma_1}(-\alpha_2\alpha_3 t)^{1/2}\right] . \tag{C9b}$$

So if $\alpha_2\alpha_3<0$, then $\hat{\mathbf{n}}=\hat{\mathbf{z}}$ is marginally stable. If $\alpha_2\alpha_3>0$, then n_x and n_y increase exponentially, so $\hat{\mathbf{n}}=\hat{\mathbf{z}}$ is unstable.

Combining the results, we expect a "textural" transition at T_t where $\alpha_3=0$. For $T>T_t$, we expect the b orientation while the a orientation is unstable. For $T_{N\text{-Sm-}A}<T<T_t$, the a orientation is marginally stable and could be realized. Note that Eqs. (C8a) and (C8b) can be combined to give the simple second-order harmonic-oscillator equation of motion:

$$\ddot{n}_{x,y} + \omega_0^2 n_{x,y} = 0 \tag{C10}$$

with $\omega_0^2=(\dot{\gamma}/\gamma_1)(-\alpha_2)\alpha_3$.

APPENDIX D: THE FLUCTUATION TORQUE FOR AN ARBITRARY ORIENTATION $\hat{\mathbf{n}}$

In this appendix we calculate, to lowest order, the torque for general $\hat{\mathbf{n}}$ on the nematic director due to the pretransitional fluctuations assuming a uniform director field. The fluctuation torque $\boldsymbol{\Gamma}_f=-\hat{\mathbf{n}}\times\delta F/\delta\hat{\mathbf{n}}$ is, using Eq. (4.9),

$$\boldsymbol{\Gamma}_f = -2\int d^3\mathbf{q}(\hat{\mathbf{n}}\times\mathbf{q})[C_\parallel(\hat{\mathbf{n}}\cdot\mathbf{q}-q_0)-C_\perp(\hat{\mathbf{n}}\cdot\mathbf{q})]S(\mathbf{q}) \ . \tag{D1}$$

We first evaluate $\boldsymbol{\Gamma}_f$ perturbatively ($\boldsymbol{\Gamma}_{\text{pert}}$). From Eq. (3.21), $\boldsymbol{\Gamma}_{\text{pert}}=\boldsymbol{\Gamma}^{(1)}_{\text{pert}}+\boldsymbol{\Gamma}^{(2)}_{\text{pert}}+\cdots$ with

$$\boldsymbol{\Gamma}^{(1)}_{\text{pert}} = \frac{1}{2\pi^3}k_B T\gamma_3\dot{\gamma}\int d^3\mathbf{q}\frac{(\hat{\mathbf{n}}\times\mathbf{q})q_x[C_\parallel(\hat{\mathbf{n}}\cdot\mathbf{q}-q_0)-C_\perp(\hat{\mathbf{n}}\cdot\mathbf{q})][(C_\parallel-C_\perp)n_y\mathbf{q}\cdot\hat{\mathbf{n}}-C_\parallel n_y q_0+C_\perp q_y]}{[A+C_\parallel(\hat{\mathbf{n}}\cdot\mathbf{q}-q_0)^2+C_\perp(\hat{\mathbf{n}}\times\mathbf{q})^2]^3} \tag{D2a}$$

and

$$\boldsymbol{\Gamma}^{2}_{\text{pert}} = \frac{1}{2\pi^3}k_B T(\gamma_3\dot{\gamma})^2\int d^3\mathbf{q}(\hat{\mathbf{n}}\times\mathbf{q})q_x^2[C_\parallel(\hat{\mathbf{n}}\cdot\mathbf{q}-q_0)-C_\perp(\hat{\mathbf{n}}\cdot\mathbf{q})] \times\left[\frac{C_\parallel n_y^2+C_\perp(n_x^2+n_z^2)}{[A+C_\parallel(\hat{\mathbf{n}}\cdot\mathbf{q}-q_0)^2+C_\perp(\hat{\mathbf{n}}\times\mathbf{q})^2]^4}-\frac{6[(C_\parallel-C_\perp)n_y\mathbf{q}\cdot\hat{\mathbf{n}}-C_\parallel n_y q_0+C_\perp q_y]^2}{[A+C_\parallel(\hat{\mathbf{n}}\cdot\mathbf{q}-q_0)^2+C_\perp(\hat{\mathbf{n}}\times\mathbf{q})^2]^5}\right] . \tag{D2b}$$

The integration range is limited by the validity condition $\Gamma_0^2\gg\alpha$ and $\Gamma_0^3(\mathbf{q})\gg\beta(\mathbf{q})$ of perturbation theory. To evaluate $\boldsymbol{\Gamma}_{\text{pert}}$, we first redefine the origin to lie at $\hat{\mathbf{n}}q_0$: $q_\parallel=\hat{\mathbf{n}}\cdot\mathbf{q}-q_0$ and $\mathbf{q}_\perp=\hat{\mathbf{n}}\times(\mathbf{q}\times\hat{\mathbf{n}})$. The dominant contribution to Eq. (D2a) is from the region around $\mathbf{q}_\parallel\simeq\mathbf{q}_\perp\simeq 0$:

$$\boldsymbol{\Gamma}^{(1)}_{\text{pert}} \cong -\frac{k_B T}{2\pi^3}\gamma_3\dot{\gamma}C_\perp n_x q_0^2\int dq_\parallel\int d^2\mathbf{q}_\perp\frac{(\hat{\mathbf{n}}\times\mathbf{q}_\perp)[C_\parallel n_y q_\parallel+C_\perp(\mathbf{q}_\perp)y]}{(A+C_\parallel q_\parallel^2+C_\perp|\mathbf{q}_\perp|^2)^3} \ . \tag{D3}$$

The integration domain of Eq. (D3) is, for n_x finite,

$$\Gamma_0^2\gg\alpha \quad\text{and}\quad \Gamma_0^3\gg\beta \ . \tag{D4}$$

Since the term $(\hat{\mathbf{n}}\times\mathbf{q}_\perp)$ is odd in $\mathbf{q}_\perp$, only the term proportional to $C_\perp(\mathbf{q}_\perp)_y$ in Eq. (D3) contributes:

$$\boldsymbol{\Gamma}^{(1)}_{\text{pert}} = -\frac{k_B T}{2\pi^3}\gamma_3\dot{\gamma}C_\perp^2 n_x q_0^2\int dq_\parallel\int d^2\mathbf{q}_\perp\frac{(\hat{\mathbf{n}}\times\mathbf{q}_\perp)(\mathbf{q}_\perp\cdot\hat{\mathbf{y}})}{(A+C_\parallel q_\parallel^2+C_\perp|\mathbf{q}_\perp|^2)^3} \ . \tag{D5}$$

Define $\boldsymbol{\rho}=\mathbf{n}\times\mathbf{q}_\perp\xi_\perp$, and $\omega=q_\parallel\xi_\parallel$. Then

$$\boldsymbol{\Gamma}^{(1)}_{\text{pert}} = \frac{k_B T\gamma_3\dot{\gamma}C_\perp^2 n_x q_0^2}{2\pi^3 A^3\xi_\parallel\xi_\perp^4}\int d^2\boldsymbol{\rho}\int d\omega\frac{\boldsymbol{\rho}\hat{\mathbf{y}}\cdot(\hat{\mathbf{n}}\times\boldsymbol{\rho})}{(1+|\boldsymbol{\rho}|^2+\omega^2)^3} \tag{D6}$$

with the boundary condition being the larger value of $r\equiv(\rho^2+\omega^2)^{1/2}$ given by

$$r_m \gg (\dot{\gamma}\tau q_0\xi_\perp n_x)^{1/4} \quad (\text{i.e., } \Gamma_0^2\gg\alpha) \tag{D7a}$$

or

$$r_m \gg \left[\frac{1}{\sqrt{3}}\dot{\gamma}\tau q_0\xi n_x\right]^{1/3} \quad (\text{i.e., } \Gamma_0^3\gg\beta) \ . \tag{D7b}$$

Going to polar coordinates

$$\Gamma^{(1)}_{\rm pert} \cong \frac{-k_B T \gamma_3 \dot\gamma C_\perp^2 n_x q_0^2}{2\pi^3 A^3 \xi_\parallel \xi_\perp^4} (\hat{\mathbf{n}}\times\hat{\mathbf{y}}) \int_{r_m}^{\infty} r^2 dr \int_{-1}^{+1} d(\cos\theta) \int_0^{2\pi} d\phi \frac{r^2 \sin^2\theta \cos^2\phi}{(1+r^2)^3} \tag{D8}$$

with $\xi^2 = \xi_\parallel^2 n_y^2 + \xi_\perp^2 (n_x^2 - n_z^2)$.

The new x axis is taken along $\hat{\mathbf{n}}\times\hat{\mathbf{y}}$ and the new z axis along $\hat{\mathbf{n}}$. After performing the integral over θ and ϕ

$$\Gamma^{(1)}_{\rm pert} \cong -\frac{1}{6\pi^2} \frac{k_B T \gamma_3 \dot\gamma n_x q_0^2 (\hat{\mathbf{n}}\times\hat{\mathbf{y}})}{A \xi_\parallel} \int_{r_m}^{\infty} \frac{r^4}{(1+r^2)^3} dr \ , \tag{D9}$$

where we used $\xi_\perp^2 = C_\perp / A$. Finally, with $\gamma_3 / A = \tau$ we get

$$\Gamma^{(1)}_{\rm pert} \simeq -\frac{1}{8\pi} \left[\frac{\dot\gamma \tau}{\xi_\parallel} \right] k_B T q_0^2 n_x (\hat{\mathbf{n}}\times\hat{\mathbf{y}}) R_{\hat{\mathbf{n}}}(\dot\gamma\tau) \ , \tag{D10}$$

where

$$R_{\hat{\mathbf{n}}}(\dot\gamma\tau) = \int_{r_m}^{\infty} \frac{r^4}{(1+r^2)^3} dr \Big/ \int_0^{\infty} \frac{r^4}{(1+r^2)^3} dr \tag{D11}$$

is a dimensionless reduction factor less than 1. We used the fact that the integral

$$\int_0^{\infty} \frac{r^4}{(1+r^2)^3} dr = 3\pi/16 \ . \tag{D12}$$

For $\dot\gamma \tau q_0 \xi n_x \ll 1$, we choose r_m given by (D7a),

$$R_{\hat{\mathbf{n}}} \simeq 1 - \left[\frac{16}{3\pi} \right] \tfrac{1}{5} [(\dot\gamma \tau q_0 \xi_\perp n_x)^{1/4}]^5 \tag{D13}$$

while for $\dot\gamma \tau_0 \xi n_x \gg 1$ we choose r_m given by (D7b),

$$R_{\hat{\mathbf{n}}} \simeq \frac{16}{3\pi} \frac{1}{[(1/\sqrt{3}) \dot\gamma \tau q_0 \xi n_x]^{1/3}} \ . \tag{D14}$$

Using Eq. (4.7) together with Eqs. (D10), (D13), and (D14) gives Eqs. (4.25) and (4.26). $\alpha_3^R(b)$ is defined in the same way as $\alpha_3^R(a)$ in Eqs. (4.12)–(4.14).

We now calculate $\Gamma^{(2)}_{\rm pert}$ given by (D2b). Once again we redefine the origin to lie at $\hat{\mathbf{n}} q_0$ and look at the dominant contributions around $\mathbf{q}_\parallel \simeq \mathbf{q}_\perp \simeq 0$:

$$\Gamma^{(2)}_{\rm pert} \simeq -\frac{1}{2\pi^3} k_B T (\gamma_3 \dot\gamma)^2 C_\perp q_0 \int dq_\parallel \int d^2\mathbf{q}_\perp (\hat{\mathbf{n}}\times\mathbf{q}_\perp)(q_x + q_0 n_x)^2 \left[\frac{C}{\Gamma_D^4} - \frac{6[C_\parallel n_y q_\parallel + C_\perp (\mathbf{q}_\perp)_y]^2}{\Gamma_D^5} \right] , \tag{D15}$$

where $\Gamma_D \equiv A + C_\parallel q_\parallel^2 + C_\perp q_\perp^2$ and $C \equiv C_\parallel n_y^2 + C_\perp (n_x^2 + n_z^2)$. The integration domain of (D15) is given by (D4). Since $(\hat{\mathbf{n}}\times\mathbf{q}_\perp)$ is odd in $\mathbf{q}_\perp$, we are left with

$$\Gamma^{(2)}_{\rm pert} \simeq -\frac{k_B T}{\pi^3} (\dot\gamma \gamma_3)^2 C_\perp q_0^2 n_x \int dq_\parallel d\mathbf{q}_\perp (\hat{\mathbf{n}}\times\mathbf{q}_\perp) q_x \left[\frac{C}{\Gamma_D^4} - \frac{6[C_\parallel n_y q_\parallel + C_\perp (\mathbf{q}_\perp)_y]^2}{\Gamma_D^5} \right] . \tag{D16}$$

We can write $q_x = q_\parallel n_x + q_\perp|_x$. This leads to two contributions to $\Gamma^{(2)}$ which we will call Γ_A and Γ_B, respectively, where

$$\Gamma_A = \frac{k_B T}{\pi^3} (\dot\gamma \gamma_3)^2 C_\perp q_0^2 n_x \int dq_\parallel \int d\mathbf{q}_\perp (\hat{\mathbf{n}}\times\mathbf{q}_\perp) q_\parallel n_x \frac{12 C_\parallel C_\perp n_y q_\parallel \mathbf{q}_\perp|_y}{\Gamma_D^5} \ . \tag{D17}$$

Only the term $q_\parallel \mathbf{q}_\perp|_y$ needs to be included since all other terms are even in $q_\parallel$. The second contribution is

$$\Gamma_B = -\frac{1}{\pi^3} k_B T (\dot\gamma \gamma_3)^2 C_\perp q_0^2 n_x \int dq_\parallel \int d\mathbf{q}_\perp (\hat{\mathbf{n}}\times\hat{\mathbf{x}}) (\mathbf{q}_\perp)_x^2 \left[\frac{C}{\Gamma_D^4} - \frac{6[C_\parallel^2 n_y^2 q_\parallel^2 + C_\perp (\mathbf{q}_\perp)_y^2]}{\Gamma_D^5} \right] . \tag{D18}$$

Only even terms in $q_\parallel$ are included and we replaced $\hat{\mathbf{n}}\times\mathbf{q}_\perp$ by $(\hat{\mathbf{n}}\times\hat{\mathbf{x}})(\mathbf{q}_\perp)_x$ because it must be odd in q_x.

Starting with Γ_A, we replace $\hat{\mathbf{n}}\times\mathbf{q}_\perp$ by $(\hat{\mathbf{n}}\times\hat{\mathbf{y}})(\mathbf{q}_\perp)_y$ since it must be odd in $(\mathbf{q}_\perp)_y$:

$$\Gamma_A = \frac{12}{\pi^3} k_B T (\dot\gamma \gamma_3)^2 C_\perp^2 C_\parallel q_0^2 n_y n_x^2 (\hat{\mathbf{n}}\times\hat{\mathbf{y}}) \int dq_\parallel \int d^2 q_\perp q_\parallel^2 (q_\perp)_y^2 / \Gamma_D^5 \ . \tag{D19}$$

Going again to polar coordinates:

$$\Gamma_A=\frac{12}{\pi^3}k_BT\frac{(\dot\gamma\tau)^2q_0^2}{\xi_\parallel}n_yn_x^2(\hat{\mathbf{n}}\times\hat{\mathbf{y}})\int_{r_m}^{\infty}r^2dr\int_{-1}^{1}d\cos\theta\int_0^{2\pi}d\varphi\left[\frac{r^4\cos^2\theta\sin^2\theta\cos^2\varphi}{(1+r^2)^5}\right]. \tag{D20}$$

Performing the angular integrals

$$\Gamma_A=\frac{1}{16\pi}k_BT\frac{(\dot\gamma\tau)^2q_0^2}{\xi_\parallel}n_yn_x^2(\hat{\mathbf{n}}\times\hat{\mathbf{y}})T_{\hat{\mathbf{n}}}(\dot\gamma\tau) \tag{D21}$$

with

$$T_{\hat{\mathbf{n}}}(\dot\gamma\tau)=\int_{r_m}^{\infty}dr\frac{r^6}{(1+r^2)^5}\Big/\int_0^{\infty}dr\frac{r^6}{(1+r^2)^5}\ . \tag{D22}$$

The function $T_{\hat{\mathbf{n}}}(\dot\gamma\tau)$ obeys $T_{\hat{\mathbf{n}}}(0)=0$ while

$$T_n(\dot\gamma\tau)\cong\left[\frac{256}{5\pi}\right]\left[\frac{\sqrt{3}}{\dot\gamma\tau q_0\xi n_x}\right] \tag{D23}$$

for $r_m\to\infty$.

Going through the same steps for Γ_B gives

$$\Gamma_B=-\frac{k_BT(\dot\gamma\tau)^2q_0^2n_x(\hat{\mathbf{n}}\times\hat{\mathbf{x}})}{8\pi\xi_\parallel}\left\{\frac{1}{3}\left[\left[\frac{C_\parallel}{C_\perp}\right]n_y^2+n_x^2+n_z^2\right]U_{\hat{\mathbf{n}}}(\dot\gamma\tau)\frac{1}{4}\left[\frac{C_\parallel}{C_\perp}n_y^2+1\right]T_{\hat{\mathbf{n}}}(\dot\gamma\tau)\right\}, \tag{D24}$$

where

$$U_{\hat{\mathbf{n}}}(\dot\gamma\tau)=\int_{r_m}^{\infty}dr\frac{r^4}{(1+r^2)^4}\Big/\int_0^{\infty}dr\frac{r^4}{(1+r^2)^4}\ . \tag{D25}$$

The function $U_n(0)=1$ and

$$U_{\hat{\mathbf{n}}}(\dot\gamma\tau)\simeq\frac{32}{\pi}\left[\frac{\sqrt{3}}{\dot\gamma\tau q_0\xi n_x}\right] \tag{D26}$$

for $r_m\gg1$.

Adding Γ_A and Γ_B gives

$$\Gamma^2_{\rm pert}=\frac{k_BT(\dot\gamma\tau)^2q_0^2}{8\pi\xi_\parallel}n_x\left\{\tfrac{1}{2}n_yn_x(\hat{\mathbf{n}}\times\hat{\mathbf{y}})T_{\hat{\mathbf{n}}}(\dot\gamma\tau)-(\hat{\mathbf{n}}\times\hat{\mathbf{x}})\left[\frac{1}{3}\frac{C}{C_\perp}U_{\hat{\mathbf{n}}}(\dot\gamma\tau)-\frac{1}{4}\left[\frac{C_\parallel}{C_\perp}n_y^2+1\right]T_{\hat{\mathbf{n}}}(\dot\gamma\tau)\right]\right\}. \tag{D27}$$

Comparing Eqs. (D10) and (D27), we see that the molecular field $\mathbf{h}$ has only $\hat{\mathbf{x}}$ and $\hat{\mathbf{y}}$ components to second order in $\dot\gamma\tau$. The first term in $\Gamma^2_{\rm pert}$ is of the form of $\Gamma^1_{\rm pert}$ except that it contains an extra factor $-\dot\gamma\tau n_xn_y$. It tends to suppress the renormalization of α_3. The second term is the frictional term discussed earlier in Eq. (4.12) in the text. For $\dot\gamma\tau q_0\xi\ll1$, the term in square brackets is positive indicating a positive friction term. For $\dot\gamma\tau q_0\xi n_x\gg1$, however, this term becomes negative. This "negative" friction suggests that for $\dot\gamma\tau q_0\xi\gg1$, there could be complicated time-dependent solutions for finite n_x. Also the stability range of $\hat{\mathbf{n}}=\hat{\mathbf{z}}$ for $\dot\gamma\tau q_0\xi\gg1$ may be very small for the same reason. As an aside we see that if we set $\hat{\mathbf{n}}=\hat{\mathbf{z}}+\delta\mathbf{n}$, $|\delta\mathbf{n}|\ll1$, we obtain $\Gamma^2_{\rm pert}=-(k_BT/12)\pi^2(\dot\gamma\tau)^2q_0^2n_x(\hat{\mathbf{n}}\times\hat{\mathbf{x}})$ which is the same as what we found in Appendix B, Eq. (B17), describing the second-order contribution to the fluctuation torque.

The region of large distortion, where $\Gamma_0^3\ll\beta$, contributes to Γ an amount Γ_s of order

$$\Gamma_s\sim\int d^3q\,|\mathbf{q}|^2cS(\mathbf{q})\ , \tag{D28}$$

where $S(\mathbf{q})\sim k_BT/(\gamma_3^2\dot\gamma^{\,2}q_x^2c)^{1/3}$ and $c\sim C_\perp\sim C_\parallel$. The integration is over the region $\Gamma_0^3\ll\beta$ or

$$(A+cq^2)^3\lesssim\gamma_3^2\dot\gamma^{\,2}q_0^2c\ . \tag{D29}$$

If we define $q_m=(\gamma_3\dot\gamma q_0/c)^{1/3}$ then

$$\Gamma_s\sim\frac{c^{2/3}k_BT}{(\gamma3\dot\gamma)^{2/3}}q_m^{13/3} \tag{D30}$$

so

$$\Gamma_s\sim\frac{q_0^2k_BT(\dot\gamma\tau)^{7/9}}{\xi(q_0\xi)^{2/3}}\ . \tag{D31}$$

For $\dot\gamma\tau q_0\xi$ of order 1, this is smaller than $\Gamma^1_{\rm pert}$ by an amount of order $(1/q_0\xi)^{13/9}$ and we can neglect Γ_s. For $\dot\gamma\tau$ of order 1, Γ_s becomes comparable to $\Gamma^1_{\rm pert}$. If we restrict ourselves to the regime $\dot\gamma\tau<1$, we can thus approximately set $\Gamma_f=\Gamma^{(1)}_{\rm pert}+\Gamma^{(2)}_{\rm pert}$. Just as for $\hat{\mathbf{n}}=\hat{\mathbf{z}}$ orientation, the second-order term $\Gamma^{(2)}_{\rm pert}$ does not contribute to the renormalization of α_3.

APPENDIX E: THE VERTEX CALCULATION FOR A SPATIALLY VARYING NEMATIC DIRECTOR

In this appendix, we compute the vertex $\langle \varphi_{\mathbf{q}} \varphi^*_{\mathbf{q}-\mathbf{k}} \rangle$. We will assume $\hat{\mathbf{n}} = \hat{\mathbf{z}} + \delta\hat{\mathbf{n}}(\mathbf{r})$ while $\psi = \varphi(\mathbf{r}) e^{iq_0 z}$ is the smectic order parameter. The nematic director is position dependent:

$$\delta\hat{\mathbf{n}}(\mathbf{r}) = \hat{\mathbf{x}} \delta n e^{ikz} . \tag{E1}$$

We start with the free energy, Eq. (3.1):

$$F = \int d^3 r \left[A |\varphi|^2 + C_{\parallel} \left| \frac{\partial \varphi}{\partial z} \right|^2 + C_{\perp} |(\nabla_{\perp} - i q_0 \delta\hat{\mathbf{n}}) \varphi|^2 \right] \tag{E2}$$

with $\nabla \equiv (\partial_x, \partial_y, 0)$. The equation of motion for $\varphi(\mathbf{r}, t)$ is, Eq. (3.3),

$$\gamma_3 \left[\frac{\partial \varphi}{\partial t} + \dot{\gamma} y \frac{\partial}{\partial x} \varphi \right] = - A \varphi + C_{\parallel} \frac{\partial^2 \varphi}{\partial z^2} + C_{\perp} [\nabla_{\perp} - i q_0 \delta\hat{\mathbf{n}}(\mathbf{r})]^2 \varphi + h(\mathbf{r}, t) . \tag{E3}$$

After applying a Fourier transform, Eq. (E3) becomes

$$\partial_t \varphi_{\mathbf{q}} - \dot{\gamma} q_x \frac{\partial}{\partial q_y} \varphi_{\mathbf{q}} = - \Gamma_0(\mathbf{q}) \varphi_{\mathbf{q}} + \frac{2 q_0 C_{\perp} \delta n q_x \varphi_{\mathbf{q}-\mathbf{k}}}{\gamma_3} + \frac{h_{\mathbf{q}}(t)}{\gamma_3} , \tag{E4}$$

where we used Eq. (E1) and where $\mathbf{k} \equiv k \hat{\mathbf{z}}$. Note that compared to Eq. (3.8), there is a new term due to the position dependence of $\delta\hat{\mathbf{n}}(\mathbf{r})$. In the limit $\delta n \to 0$, we can neglect this term after which we recover Eq. (3.14):

$$\varphi^0_{\mathbf{q}}(t) = \int_{-\infty}^{t} dt' \exp[-(t-t') \tilde{\Gamma}(\mathbf{q})] h_{\mathbf{q}}(t') / \gamma_3 \tag{E5}$$

with the operator

$$\tilde{\Gamma}(\mathbf{q}) = \frac{A + C_{\parallel} q_z^2 + C_{\perp}(q_x^2 + q_y^2)}{\gamma_3} - \dot{\gamma} q_x \frac{\partial}{\partial q_y} . \tag{E6}$$

We can get the lowest-order correction to (E5) by replacing $\varphi_{\mathbf{q}-\mathbf{k}}$ with $\varphi^0_{\mathbf{q}-\mathbf{k}}$ in Eq. (E4) and then replacing

$$h_{\mathbf{q}}(t) \to h_{\mathbf{q}}(t) + 2 q_0 C_{\perp} \delta n q_x \varphi^0_{\mathbf{q}-\mathbf{k}}(t) \tag{E7}$$

in Eq. (E5). The matrix element is now, to lowest order,

$$\langle \varphi_{\mathbf{q}} \varphi^*_{\mathbf{q}-\mathbf{k}} \rangle \simeq 2 q_0 C_{\perp} \delta n q_x \int_{-\infty}^{t} dt' \exp[-(t-t') \tilde{\Gamma}(\mathbf{q}) \gamma^3] \times \langle |\varphi^0_{\mathbf{q}-\mathbf{k}}(t)|^2 \rangle . \tag{E8}$$

For $t \to \infty$,

$$\langle \varphi_{\mathbf{q}} \varphi^*_{\mathbf{q}-\mathbf{k}} \rangle \simeq 2 q_0 C_{\perp} \delta n q_x [\tilde{\Gamma}(\mathbf{q})]^{-1} S(\mathbf{q} - \mathbf{k} + q_0 \hat{\mathbf{z}}) . \tag{E9}$$

This can be written as a differential equation:

$$\left[\Gamma_0(\mathbf{q}) - \dot{\gamma} q_x \frac{\partial}{\partial q_y} \right] \langle \varphi_{\mathbf{q}} \varphi^*_{\mathbf{q}-\mathbf{k}} \rangle \simeq 2 q_0 C_{\perp} \delta n q_x S(\mathbf{q} - \mathbf{k} + q_0 \hat{\mathbf{z}}) \tag{E10}$$

which is Eq. (4.36).

We can solve Eq. (E10) iteratively in $\dot{\gamma} q_s \partial / \partial q_y$:

$$\langle \varphi_{\mathbf{q}} \varphi_{\mathbf{q}-\mathbf{k}} \rangle^* = \sum_{n=0}^{\infty} \langle \varphi_{\mathbf{q}} \varphi^*_{\mathbf{q}-\mathbf{k}} \rangle_n , \tag{E11}$$

where

$$\langle \varphi_{\mathbf{q}} \varphi^*_{\mathbf{q}-\mathbf{k}} \rangle_0 = 2 q_0 C_{\perp} \delta n_x \frac{q_x S(\mathbf{q} - \mathbf{k} + q_0 \hat{\mathbf{z}})}{\Gamma_0(\mathbf{q})} \tag{E12}$$

and

$$\langle \varphi_{\mathbf{q}} \varphi^*_{\mathbf{q}-\mathbf{k}} \rangle_n = \left[\frac{1}{\Gamma_0(\mathbf{q})} \dot{\gamma} q_x \frac{\partial}{\partial q_y} \right]^n \langle \varphi_{\mathbf{q}} \varphi^*_{\mathbf{q}-\mathbf{k}} \rangle_0 . \tag{E13}$$

We only need the derivative $(\partial^2/\partial k^2)(\partial/\partial n) \langle \varphi_{\mathbf{q}} - \varphi^*_{\mathbf{q}-\mathbf{k}} \rangle$ to compute K_3^R in Eq. (4.35). From Eqs. (E11)–(E13),

$$\frac{\partial^2}{\partial k^2} \frac{\partial}{\partial n} \langle \varphi_{\mathbf{q}} \varphi^*_{\mathbf{q}-\mathbf{k}} \rangle = 2 q_0 C_{\perp} q_x \sum_{n=0}^{\infty} \left[\frac{1}{\Gamma_0(\mathbf{q})} \dot{\gamma} q_x \frac{\partial}{\partial q_y} \right]^n \times \frac{1}{\Gamma_0(\mathbf{q})} \frac{\partial^2}{\partial q_z^2} S(\mathbf{q} - q_0 \hat{\mathbf{z}}) . \tag{E14}$$

Recall that S itself is a power series in $\dot{\gamma}$ [Eq. (B2)],

$$S(\mathbf{q} - q_0 \hat{\mathbf{z}}) = \frac{1}{(2\pi)^3} \sum_{n=0}^{\infty} \left[\frac{\dot{\gamma}}{\Gamma_0(\mathbf{q})} q_x \frac{\partial}{\partial q_y} \right]^n \frac{k_B T}{\gamma_3 \Gamma_0(\mathbf{q})} . \tag{E15}$$

Collecting terms of the same order in $\dot{\gamma}$ gives

$$\frac{\partial^2}{\partial k^2} \frac{\partial}{\partial n} \langle \varphi_{\mathbf{q}} \varphi^*_{\mathbf{q}-\mathbf{k}} \rangle = \frac{q_0 C_{\perp}}{4\pi^3} \frac{k_B T q_x}{\gamma_3^2 \Gamma_0(\mathbf{q})} \left\{ \frac{1}{\Gamma_0} \frac{\partial^2}{\partial q_z^2} \frac{1}{\Gamma_0} + \frac{(\dot{\gamma} q_x)}{\gamma_3} \left[\frac{\partial}{\partial q_y} \left[\frac{1}{\Gamma_0} \frac{\partial^2}{\partial q_z^2} \frac{1}{\Gamma_0} \right] + \frac{\partial^2}{\partial q_z^2} \left[\frac{1}{\Gamma_0} \frac{\partial}{\partial q_y} \frac{1}{\Gamma_0} \right] \right] + (\dot{\gamma} q_x)^2 \left[\frac{\partial}{\partial q_y} \left[\frac{1}{\Gamma_0} \frac{\partial}{\partial q_y} \frac{\partial^2}{\partial q_z^2} \frac{1}{\Gamma_0} \right] + \frac{\partial}{\partial q_y} \frac{\partial^2}{\partial q_z^2} \left[\frac{1}{\Gamma_0} \frac{\partial}{\partial q_y} \frac{1}{\Gamma_0} \right] + \frac{1}{\gamma_3} \frac{\partial^2}{\partial q_z^2} \left[\frac{1}{\Gamma_0} \frac{\partial}{\partial q_y} \frac{1}{\Gamma_0} \frac{\partial}{\partial q_y} \frac{1}{\Gamma_0} \right] \right] + O(\dot{\gamma}^3) \right\} . \tag{E16}$$

The term in $\dot{\gamma} q_x$ is odd in q_y and cannot contribute to K_3^R. The first term gives Eq. (4.41). The term in $(\dot{\gamma} q_x)^2$ gives Eq. (4.42).

APPENDIX F: NORMAL STRESSES IN NEMATIC LIQUID CRYSTALS

As mentioned in the Introduction, if a non-Newtonian fluid is subjected to shear flow then this inevitably generates extensional flow as well. The extensional flow is due to the appearance of the normal-stress differences $\sigma = \sigma_{xx} - \sigma_{yy}$ and $\sigma' = \sigma_{yy} - \sigma_{zz}$ in the stress tensor which are zero for Newtonian flow. It is common to parametrize σ and σ' as

$$\sigma = \psi_1 \dot{\gamma}^2 , \tag{F1a}$$

$$\sigma' = \psi_2 \dot{\gamma}^2 , \tag{F1b}$$

with ψ_1 and ψ_2 the so-called normal-stress coefficients. In general $\psi_1 \gg \psi_2$, while they both depend on $\dot{\gamma}$. In the limit $\dot{\gamma} \to 0$, ψ_1 and ψ_2 go to a constant. These normal stresses are in fact responsible for the unusual flow properties of polymeric fluids.

For fluids close to a critical point we can estimate the singular temperature dependence of σ (or σ') from dynamical scaling. The components of the stress tensor have the dimension of a free-energy density. Near $T_{N\text{-Sm-}A}$, the only scaling quantity with those units is the free-energy density $k_B T / \xi_\parallel \xi_\perp^2$ itself. From dynamical scaling it then follows that

$$\sigma(\dot{\gamma}) \propto \left[\frac{k_B T}{\xi_\parallel \xi_\perp^2} \right] g(\dot{\gamma}\tau) , \tag{F2}$$

where $g(x)$ is an unknown scaling function with $g(\infty) = 0$. Since in the limit $\dot{\gamma} \to 0$, σ is proportional to $\dot{\gamma}^2$ we conclude that for small x, $g(x) \sim x^2$ so

$$\psi_{1,2} \propto \left[\frac{k_B T \tau^2}{\xi_\parallel \xi_\perp^2} \right] . \tag{F3}$$

Since, within dynamical scaling, $\tau(\xi) \sim \xi^{3/2}$ one does not expect a very strong temperature dependence for ψ_1 but this will depend on the precise relation between τ and $\xi_\parallel$ and $\xi_\perp$, which is not known.

We can check this result with a (heuristic) microscopic calculation of the normal stresses. Normal stresses are due to the elastic distortion of the fluctuation clusters. Assume that at time $t = 0$, a fluctuation cluster $\psi(\mathbf{r}, t)$ appears with $\hat{\mathbf{n}} = \hat{\mathbf{z}}$. The time-dependent free-energy density $f(\mathbf{r}, t)$ of the cluster is

$$f(\mathbf{r}, t) \cong \left[A + C_\parallel \frac{\partial^2}{\partial z^2} + C_\perp \left[\frac{\partial^2}{\partial x^2} + \frac{\partial^2}{\partial y^2} \right] \right] \times \langle |\psi(\mathbf{r}, t)|^2 \rangle . \tag{F4}$$

Under shear flow, the cluster will get distorted. The elastic energy cost $\delta f(\mathbf{r}, t)$ of the distortion

$$\delta f(\mathbf{r}, t) = f(\mathbf{r} + \dot{\gamma} y t \hat{\mathbf{x}}, t) - f(\mathbf{r}, t) \approx \dot{\gamma} y t \frac{\partial f}{\partial x}(\mathbf{r}, t) \tag{F5}$$

for small Deborah number. We can think of δf as the work done by a force $F = \partial f / \partial x$ during a displacement $X = \dot{\gamma} t y$. The component σ_{xx} of the stress tensor is the average of the restoring force F and displacement X over all clusters:

$$\sigma_{xx} \propto \langle \langle FX \rangle \rangle . \tag{F6}$$

In our case, this gives

$$\sigma_{xx} \propto \left\langle \left\langle \dot{\gamma} t y \frac{\partial f}{\partial x} \right\rangle \right\rangle \tag{F7}$$

with an average over t and $\mathbf{r}$. The same argument also gives $\sigma_{yy} = \sigma_{zz} \cong 0$. After going to momentum space and averaging over time, one finds that

$$\sigma_{xx} \propto \frac{1}{T} \int_0^T dt (\dot{\gamma} t) \int d^3 q q_x \frac{\partial}{\partial q_y} [(A + C_\parallel q_z^2 + C_\perp q_\perp^2) \times \langle |\psi_{\mathbf{q}}(t)|^2 \rangle] \tag{F8}$$

with $T \to \infty$. Using the fact that $\langle |\psi_{\mathbf{q}}(t)|^2 \rangle$ is proportional to $\exp - t / \tau(\mathbf{q})$ gives

$$\sigma_{xx} \propto \int d^3 \mathbf{q} \frac{(\dot{\gamma} \gamma_3)}{\Gamma_0(\mathbf{q})} q_x \frac{\partial}{\partial q_y} [(A + C_\parallel q_z^2 + C_\perp q_\perp^2) S(\mathbf{q})] . \tag{F9}$$

If we use the perturbation expansion for $S(\mathbf{q})$ then only terms of symmetry $q_x q_y$ survive. In "real space" this corresponds to the $l = 1$ spherical harmonic of the density correlation function which has xy/r^2 symmetry. The only term of that form in Eq. (3.21) is the one proportional to $\alpha(\mathbf{q})$. The resulting integral reproduces (unsurprisingly) the dynamical scaling result for ψ_1. Within our heuristic argument, $\psi_2 = 0$.[36]

---

[1] O. Reynolds, Philos. Mag. **20**, 46 (1885).

[2] D. J. Evans, H. J. M. Hanley, and S. Hess, Phys. Today **37**(1), 26 (1984), and references therein. For an introduction to the subject of polymeric fluids, see R. Byron Bird, R. C. Armstrong, and Ole Hassager, *Dynamics of Polymeric Liquids,* 2nd ed. (Wiley-Interscience, New York, 1987), Vol. 1.

[3] We point out that relaxation rates (τ) are proportional to the solution viscosity η. Therefore, in principle, one may increase τ in a simple fluid by approaching the glass transition where η increases exponentially. For example, in glycerol just above $T_G = 184$ K, η increases by many orders of magnitude. The accompanying frictional heating $\eta \dot{\gamma}^2$ would, however, be prohibitive for controlled experiments.

[4] For a survey of complex fluids (macromolecular liquid) systems see *Physics of Complex and Supermolecular Fluids,* edited by S. A. Safran and N. A. Clark (Wiley, New York, 1987); and *Macromolecular Liquids,* edited by C. R. Safinya, S. A. Safran, and P. A. Pincus (Materials Research Society, Pittsburgh, 1990), Vol. 177.

[5] N. A. Clark and B. J. Ackerson, Phys. Rev. Lett. **44**, 1005 (1980); B. J. Ackerson and N. A. Clark, Physica **83A**, 221

(1983).

[6]See, for instance; R. B. Bird and C. F. Curtiss, Phys. Today **37**(1), 36 (1984); and R. Byron Bird, R. C. Armstrong, and Ole Hassager, Ref. 2.

[7]P. G. DeGennes, *Scaling Concepts in Polymer Physics* (Cornell University Press, Ithaca, 1979).

[8]P. C. Hohenberg and B. I. Halperin, Rev. Mod. Phys. **49**, 435 (1977).

[9]A. Onuki and K. Kawasaki, Ann. Phys. (N.Y.) **121**, 456 (1979).

[10]D. Beysens, M. Gbadamassi, and B. Moncef-Bouanz, Phys. Rev. A **28**, 2491 (1983); A. Onuki, K. Yamazaki, and K. Kawasaki, Ann. Phys. (N.Y.) **131**, 217 (1981).

[11]P. G. DeGennes, *The Physics of Liquid Crystals* (Oxford University Press, London, 1974).

[12]C. R. Safinya, E. B. Sirota, and R. Plano, Phys. Rev. Lett. (to be published); C. R. Safinya, E. B. Sirota, R. Plano, and R. F. Bruinsma, J. Phys. Condens. Matter **2**, SA365 (1990); C. R. Safinya, E. B. Sirota, R. Plano, and N. Lei, in *Macromolecular Liquids,* edited by C. R. Safinya, S. A. Safran, and P. A. Pincus, MRS Symposia Proceedings No. 177 (Materials Research Society, Pittsburgh, 1990), p. 165.

[13]J. Als-Nielsen, R. J. Birgeneau, M. Kaplan, J. D. Litster, and C. R. Safinya, Phys. Rev. Lett. **39**, 352 (1977); D. Davidov, C. R. Safinya, M. Kaplan, S. S. Dana, R. Schaetzing, R. J. Birgeneau, and J. D. Litster, Phys. Rev. B **19**, 1657 (1979).

[14]B. M. Ocko, R. J. Birgeneau, J. D. Litster, and M. E. Newbert, Phys. Rev. Lett. **52**, 208 (1984); C. W. Garland, M. Meichle, B. M. Ocko, A. R. Kortan, C. R. Safinya, L. J. Yu, J. D. Litster, and R. J. Birgeneau, Phys. Rev. A **27**, 3234 (1988); K. K. Chan, P. S. Pershan, L. B. Sorensen, and F. Hardouin, *ibid.* **34**, 1420 (1986).

[15]P. G. de Gennes, Mol. Cryst. Liq. Cryst. **34**, 91 (1976); Sriram Ramaswamy, Phys. Rev. A **29**, 1506 (1984); G. H. Fredrickson, J. Chem. Phys. **85**, 5306 (1986); M. E. Cates and S. T. Milner, Phys. Rev. Lett. **62**, 1856 (1989); P. D. Olmsted and P. Goldbart (unpublished); R. G. Larson (unpublished).

[16]W. L. McMillan, Phys. Rev. A **17**, 1419 (1973).

[17]Experimentally, the fluctuations are more accurately described by a modified Ornstein-Zernike form with a small transverse quartic term $c\xi_1^4(q_x^2+q_y^2)^2$ added to the denominator of Eq. (1.1). This term has been attributed to director fluctuations (see Refs. 14 and 15). For the sake of simplicity we drop this term.

[18]For a review see T. C. Lubensky, J. Chem. Phys. Phys.-Chim. Biol. **80**, 31 (1983). The experiments of Chan *et al.* (Ref. 14) suggest that the divergent phase fluctuations of the smectic-A order parameter are responsible for the anisotropic length scales of the N–Sm-A transition.

[19]L. Leger and A. Martinet, J. Phys. (Paris) Colloq. **37**, C63-89 (1976); C. C. Huang *et al.*, Phys. Rev. Lett. **33**, 400 (1974); M. Delaye, J. Phys. (Paris) Colloq. **37**, C3-99 (1976).

[20]H. Birecki and J. D. Litster, Mol. Cryst. Liq. Cryst. **42**, 33 (1977); also see Ref. 13, Davidov *et al.*

[21]J. L. Ericksen, Arch. Ration. Mech. Anal. **4**, 231 (1960); **9**, 371 (1962); Appl. Mech. Rev. **20**, 1029 (1967).

[22]F. M. Leslie, Quart. J. Mech. Appl. Math. **19**, 357 (1966).

[23]O. Parodi, J. Phys. (Paris) **31**, 581 (1970).

[24]D. Foster, T. C. Lubensky, P. C. Martin, J. Swift, and P. S. Pershan, Phys. Rev. Lett. **26**, 1016 (1971); P. C. Martin, O. Parodi, and P. J. Pershan, Phys. Rev. A **6**, 2401 (1972).

[25]M. Miesowicz, Nature (London) **158**, 27 (1946).

[26]W. L. McMillan, Phys. Rev. A **9**, 1720 (1974).

[27]F. Janig and F. Brochard, J. Phys. (Paris) **35**, 301 (1974).

[28]P. G. DeGennes, Solid State Commun. **10**, 753 (1972).

[29]W. L. McMillan, Phys. Rev. A **6**, 936 (1972).

[30]K. Sharp, T. Carlsson, S. T. Lagerwall, and B. Stebler, Mol. Cryst. Liq. Cryst. **66**, 199 (1981); P. Pieranski and E. Guyon, Phys. Rev. A **9**, 404 (1974).

[31]P. Pieranski and E. Guyon, Phys. Rev. Lett. **32**, 924 (1974).

[32]In instructive papers W. Helfrich [J. Chem. Phys. **50**, 100 (1969); **53**, 2267 (1970)] outlined a molecular model to explain the flow alignment of the nematic director in the x-y shear plane which is observed at high temperature in the nematic phase where the effect of smectic-A fluctuations can be ignored. The model is based on ellipsoidal shaped molecules and relates the Leslie parameters α_2 and α_3 to the dimensions of the molecule. α_2 is found to be negative. For most shapes α_3 is negative.

[33]P. G. De Gennes, Solid State Commun. **10**, 753 (1972).

[34]A. Schmid, Phys. Rev. **180**, 527 (1969).

[35]See, e.g., I. S. Gradshteyn and I. M. Ryzhik, *Tables of Integrals, Series, and Products* (Academic, New York, 1980), p. 317.

[36]Ch. Gähwiller, Phys. Rev. Lett. **28**, 1554 (1972).